Critical Reviews in Environmental Science and Technology, 45:101–166, 2015

ISSN: 1064-3389 print / 1547-6537 online
DOI: 10.1080/10643389.2013.829981

Remote Sensing for Monitoring Surface Water Quality Status and Ecosystem State in Relation to the Nutrient Cycle: A 40-Year Perspective

NI-BIN CHANG, SANAZ IMEN, and BENJAMIN VANNAH
Department of Civil, Environmental, and Construction Engineering, University of Central Florida, Orlando, FL, USA

*Delineating accurate nutrient fluxes and distributions in multimedia environments requires the integration of vast amounts of information. Such nutrient flows may be related to atmospheric deposition, agricultural runoff, and urbanization effect on surface and groundwater systems. Two types of significant undertakings for nutrient management have been in place for sustainable development. While many environmental engineering technologies for nutrient removal have been developed to secure tap water sources and improve the drinking water quality, various watershed management strategies for eutrophication control are moving to highlight the acute need for monitoring the dynamics and complexities that arise from nutrient impacts on water quality status and ecosystem state, both spatially and temporally. These monitoring methods and data are associated with local point measurements, air-borne remote sensing, and space-borne satellite images of spatiotemporal nutrient distributions leading to the generation of accurate environmental patterns. Within this context, several key water quality constituents, including total nitrogen, total phosphorus, chlorophyll-*a *concentration, colored dissolved organic matter (dissolved organic carbon or total organic carbon), harmful algal blooms (e.g., cyanobacterial toxins or microcystin concentrations), and descriptors of ecosystem states, such as total suspended sediment (or turbidity), transparency (e.g., Secchi disk depth), and*

Address correspondence to Ni-Bin Chang, Department of Civil, Environmental, and Construction Engineering, University of Central Florida, 4000 Central Florida Blvd, Orlando, FL 32816, USA. E-mail: nchang@mail.ucf.edu

Color versions of one or more of the figures in the article can be found online at www.tandfonline.com/best.

temperature, will be of major concern. Considering the advancements, challenges, and accomplishments related to remote sensing technologies in the past four decades, we present a thorough literature review of contemporary state-of-the-art technologies of remote sensing platforms and sensors that may be employed to support essential scientific missions, and provide an in-depth discussion and new insight into various inversion methods (or models) to improve the estimation accuracy. In this study, the spectrum of these remote sensing technologies and models is first divided into groups based on chronological order associated with different platforms and sensors, although some of them may be subject to mission-oriented arrangements. Case-based and location-based studies were cited, organized, and summarized to further elucidate tracks of application potential that support future, forward-looking, cost-effective, and risk-informed nutrient management plans. The comprehensive reviews presented here should echo real-world observational evidence by using integrated sensing, monitoring, and modeling techniques to improve environmental management, policy analysis, and decision making.

KEY WORDS: remote sensing, nutrient management, water quality management, sustainable management

1. INTRODUCTION

During the 20th century, widespread global changes occurred due to climatic variations, shifting demographics, population migration, rapid urbanization, and economic development. Under global change impacts, many surface and groundwater systems were contaminated by treated or untreated wastewater discharged with high nutrient contents, nutrient-laden agricultural runoffs, landfill leachate disposal with high nutrient concentrations, and increasing use of fertilizer in residential communities (Chang et al., 2010a; Chang et al., 2010b). With the impact of industrialization, the atmospheric deposition of nitrogen can also play a key role in the overall nitrogen budgets of terrestrial (e.g., Adirondack region of New York State) and coastal (e.g., Chesapeake Bay) ecosystems (U.S. Environmental Protection Agency [EPA], 2002). Whereas the water quality issues are related to the presence of both dissolved and particulate nitrogen (N) species directly discharged from municipal and agricultural sources into aquatic environments, the atmospheric pollutants also contribute to N deposition derived mainly from nitrogen oxides (NO_X) and ammonia (NH_3) emissions at industrial sources. Yet trends in dissolved and suspended phosphorous (P) levels through agricultural fertilization and manure management in watersheds are also a concern in nutrient

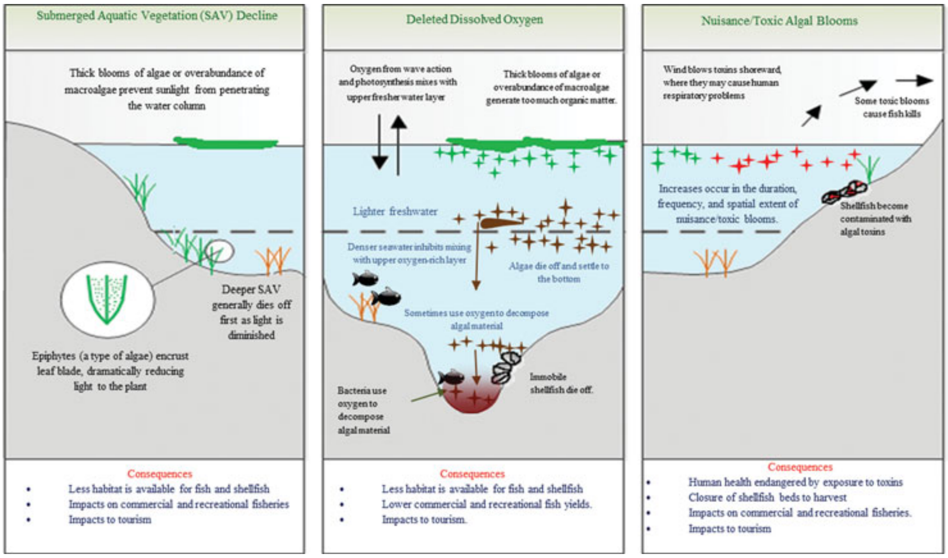

FIGURE 1. Nutrient effects on changing water quality status and ecosystem state (adapted from U.S. Environmental Protection Agency, 2002).

management. Excessive nutrients, which may be represented as total nitrogen (TN) and total phosphorus (TP) levels, in natural water systems have proven to cause high levels of algae production in aquatic environments. The process of phytoplankton growth that consumes excess nutrients in a water body can also be related to changing water quality constituents, including dissolved oxygen (DO), pH, chlorophyll-*a*, forms of organic carbon (colored dissolved organic carbon [CDOM], dissolved organic carbon [DOC], or total organic carbon [TOC]), or can alter descriptors of water state such as Secchi disk depth (transparency; SDD), temperature, and turbidity (total suspended sediment [TSS]). All of these constituents and factors may collectively cause changes in terms of water quality status and ecosystem state, such as acidification of lakes and streams, eutrophication of estuaries and near coastal waters, nitrogen saturation of watersheds, changes in soil chemistry, and increase in groundwater nitrate concentrations. These eutrophication conditions might result in the formation of harmful algal blooms (HABs; Figure 1), some of which are toxic due to the presence of *Microcystis*, a cyanobacteria that produces the hepatotoxin microcystin. Phycocyanin, a pigment that all cyanobacteria contain (World Health Organization, 1999), has been shown to share a positive correlation with microcystin levels (Rinta-Kanto et al., 2009).

Elevated levels of N and P concentrations in environmental systems can cause public health problems, such as blue baby syndrome (methemoglobinemia) caused by nitrate pollution (Knobeloch et al., 2000) and liver cancer due to the presence of cyanobacteria toxin (Falconer et al., 1993, 1996; Chorus and Fastner, 2001). Further, nutrient levels are major concern for water treatment plants using groundwater, lake water, or coastal water as a tap water source. In addition, high levels of N and P may impair or destroy environmentally sensitive ecosystem habitats, such as the loss of submerged aquatic vegetation due to eutrophication (e.g., tape grass [*Vallisneria Americana*] in Indian River Lagoon; Alleman, 2012). Consequently, continuous and effective environmental monitoring of water availability and quality in relation to nutrient cycle has become a focus worldwide.

Understanding changing nutrient distributions in coupled human and natural systems is subject to many complex, intertwined, large-scale drivers such as climatic trends, land use-land cover patterns, ecosystem heterogeneity, hydrographic features, water infiltration and runoff, and others. To date, however, no sophisticated hydrological model is capable of tackling all relevant biogeochemcial processes in association with the complicated nutrient cycle as a whole, driven by the hydrological cycle. With such systemic concerns, nutrient management has become one of the 12 grand engineering challenges in the 21st century identified by the National Academy of Engineering in 2008 in the United States (National Academies, 2008). Nutrient management efforts, such as the Chesapeake Watershed study in the 1990s, the Great Lakes Restoration Initiative through the 2000s, and the Comprehensive Everglades Restoration Plan (CERP) in early 2000s have continuously become national foci in various comprehensive environmental management plans such as the recent emergence of the Florida Numeric Nutrient Criteria—62-302.530(47)(b), Florida Administrative Code—in 2012. Over the past few decades, leaps in remote sensing technologies have enabled unprecedented observations and measurements achieving fundamental advances in monitoring water availability and quality (Chang et al., 2010c). Earth observation data have become essential for making forward-looking, risk-informed, and cost-effective decision making. Such advancements provide interactive functions to support new avenues for model calibration and validation in the nexus of environmental systems analysis and risk assessment.

Although many studies have reviewed the applications of remote sensing in estimating hydrological parameters (e.g., evapotranspiration, rainfall, snowfall), relatively few assessed the applications of remotely sensed data in determining water quality status (e.g., TSS, TN, TP) and ecosystem state (e.g., chlorophyll-*a* and HABs/microcystins; Glasgow et al., 2004). Limited reviews were separately conducted for the individual study of suspended sediments across remotely sensed spectral radiance (Curran and Novo, 1988); grouped study of suspended sediments, algae, aquatic vascular plants, and temperature (Ritchie et al., 2003); and grouped study of suspended sediments, chlorophyll-*a* concentration, and SDD (Liu et al., 2003). As the national need for this information grows, the Committee of Hydrological Science in the National Research Council has produced *Integrating Multiscale Observations* *of U.S. Waters* (National Research Council, 2008) to promote the field of remote sensing (Chang and Hong, 2012). Evolving information required for sound nutrient management faces barriers not only related to a shortage of information due to insufficient sensing, monitoring, and modeling capacity to estimate nutrient budget in terrestrial and coastal watersheds, but also linked with the challenge to organize and disseminate the available information in ways that illuminate alternative pathways of nutrient distributions. With the advent of remote sensing and sensor network technologies, however, come the logical consequences of identifying the hot moments and spots of nutrient pollution to aid in decision making nationwide.

Remote sensing methods can provide information on both spatial and temporal distributions of key variables. These methods can be ground-based (e.g., in situ sensor networks), or based on aircraft or satellites. To deal with these nutrient management issues with the aid of remote sensing technologies, we should implement system thinking to (a) adopt integrated approaches with multiscale observations, (b) use the best available science, (c) apply risk management methods and tools, and (d) apply ecosystem-based approaches. Thus, our aim is to provide an up-to-date, thorough review of multiscale remote sensing technologies applied over the past four decades for monitoring water quality status and ecosystem state in relation to nutrient flows and distribution. We include a comprehensive discussion of future perspectives and incorporate integrated, near real-time remote sensing monitoring systems and state-of-the-art informatics systems for meeting the future demand of hydrological monitoring, data management, and dissemination. This review is limited to six major water quality parameters (TSS, chlorophyll-*a*, nutrients, TOC, temperature, and microcystin), deemed as the top water pollution indices related to public health, eutrophication, and loss of ecosystem habitat in different water bodies in the United States (U.S. EPA, 2009), to present a canonical metrics in connection to intertwined water quality and ecosystem assessment.

2. REMOTE SENSING PLATFORMS AND SENSORS

All substances in natural systems and the built environments may absorb, transmit, scatter, emit, and reflect portions of the electromagnetic spectrum (i.e., sunlight). The amount of light that an object may reflect is a function of a specific frequency or wavelength. Objects with differing spectral properties yield spectral curves that are not as comparable, thus facilitating the distinction between the materials. Instruments that detect reflected natural radiation (typically sunlight) are classified as passive sensing systems and active sensing systems. Active sensing systems generate pulses of electromagnetic radiation that are detected by the sensor as they reflect off the target; passive sensing systems simply measure the natural reflectance off the

TABLE 1. Regions of the electromagnetic spectrum common to remote sensing (K band is split due to strong absorption in water vapor)

Band	Band range or wavelength (cm)
L	30–15
S	15–8
C	8–4
X	4–2.5
K	2.5–1.7 and 1.2–0.75
Microwave (MW)	10–0.01
Infrared	$0.01–7 \times 10^{-5}$
Visible Light	7×10^{-5} to 4×10^{-5}
Ultraviolet	4×10^{-5} to 10^{-7}

target. Satellite platforms utilizing passive remote sensing technology need to maintain sun-synchronous orbits to support the effective remote sensing.

Detection of electromagnetic radiation is the foundation for determining water quality status and ecosystem state through remote sensing. Thus, the application of electromagnetic radiation detection can be extended to monitoring surface waters because the backscattering characteristics of water depend on the types and concentrations of substances in the water (Shubha, 2000). The main spectral bands of interest for remote sensing in water bodies are visible (VIS), infrared (IR), and microwave (MW; Richards, 1986; Schultz, 1988). Commonly used spectral bands associated with their wavelength (Table 1) have distinct detection instruments used in remote sensing (Table 2). The ability to recognize materials with similar spectral properties in aerial images is limited because the slope angles and directions affect the brightness of each surface material from one location to another. The band ratio of two spectral bands is applied to remove these effects by dividing the

TABLE 2. Remote sensing band categories and their types of instruments (Goodman, 1994)

Band	Wavelength	Types of instruments
Radar	1–30 cm	SLAR/SAR
Passive microwave	2–8 mm	Radiometers
Thermal infrared (TIR)	8–14 μm	Video cameras and line scanners
Mid-band infrared (MIR)	3–5 μm	Video cameras and line scanners
Near infrared (NIR)	1–3 μm	Film, video cameras
Visual	350–750 nm	Film, video cameras and spectrometers
Ultraviolet	250–350 nm	Film, video cameras and line scanners

Note. SLAR: Side-Looking Airborne Radar; SAR: Synthetic Aperture Radar.

brightness value in one band to the value in the second band, which cancels out the contribution of shadowing and shading because it is constant in all image bands (Smith, 2012). An example of reflectance spectra from different types of waters (Figure 2) shows the effects of water column and bottom on reflectance, and the bottom reflectance of different water constituents (and Mobley, 2003; Mobley et al., 2004; Shubha, 2000; Albert). Morel and Prieur (1977) classified waters into two categories based on their optical purposes. Case 1 waters are those in which optical properties are mainly determined by phytoplankton and covarying materials of biological origin (particulate and dissolved), whereas Case 2 waters are influenced not only by phytoplankton and related material, but also by other substances (notably suspended inorganic particles and CDOM) that vary independently of phytoplankton (Lapucci et al., 2012). Case 2 conditions are usually seen in coastal waters, enclosed seas, and shallow tidal seas as a result of resuspension of bottom sediments (Robinson, 2004).

Common passive remote sensor types that measure the spectral intensity for multiple distributions of wavelengths include spectrometers, radiometers, imaging radiometers, and spectroradiometers. Spectrometers detect electromagnetic radiation through the use of filters, prisms, gratings, or mirrors to disperse the radiation to measure and analyze the spectral components. Radiometers measure the intensity of electromagnetic radiation over a specified portion of the electromagnetic spectrum. Imaging radiometers generate a two-dimensional array of spectral intensity values to form an image for specific analysis. In particular, spectroradiometers are a combination of spectrometers and radiometers that can measure the spectral intensity for multiple distributions of wavelengths.

Sensors detecting spectral signatures in the visible and infrared spectrum only work well in the absence of clouds or smoke, which can obstruct the optical remote sensing images and limit applications in regions prone to bad weather. In all conditions, environmental monitoring and earth-resource mapping often require long-standing, broad-area imaging at high resolutions. Microwaves are able to pass through clouds and smoke, which provide meaningful readings, even under cloud cover, and active remote sensing with C, L, or X bands. The radiation detected by active remote sensors is produced by the remote sensing platform itself and is reflected back by the target. Radar not affected by lighting conditions is a well-known example of an active remote sensor in which a transmitter is used to pulse radio and microwaves at a target, and a receiver captures the reflected and backscattered radiation. This type of remote sensing system can provide images in all weather conditions with high resolution due to the use of microwave wavelength. Scatterometers are a specific type of radar that measure backscattered radiation generated by high frequency microwave radar. In comparison, synthetic aperture radar (SAR) works by collecting the echo returns from many radar pulses and processing them into a single radar image to take advantage

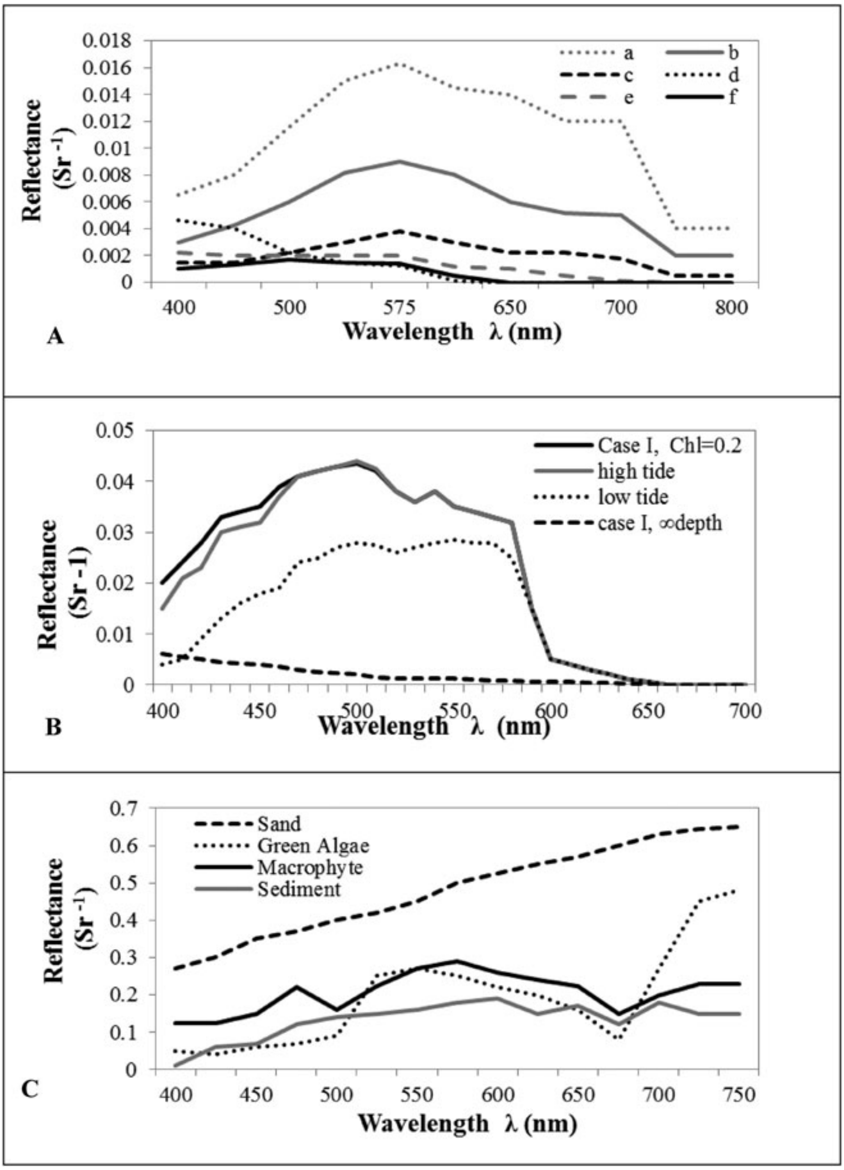

FIGURE 2. (A) Reflectance spectra of different types of waters. (a) Waters with very high sediment and Gelbstoff concentrations, (b) high sediment and Gelbstoff concentration, (c) moderate sediment and Gelbstoff concentration, (c) moderate sediment and Gelbstoff concentration, (c) moderate sediment and Gelbstoff with some phytoplankton, (d) clear water, (e) waters with moderate chlorophyll and sediment concentration, (f) waters with moderate chlorophyll-*a* concentration. Time series plots of a, b, c, and e show Case 2; d and f show Case 1 (Shubha, 2000). (B) The effect of water column and bottom on reflectance spectra. Reflectance is significantly related to the tide, which at low tide it is less than the reflectance in Case 1. The infinite depth is much smaller than the curve for 5 m depth (Mobley et al., 2004). (C) Bottom reflectance spectra for four different water constituents (Albert and Mobley, 2003).

of the long-range propagation characteristics of radar signals and the complex information processing capability of modern digital electronics to provide high resolution imagery. Scatterometers can be applied to determine surface wind speeds over an ocean (Naderi et al., 1991), and SAR can be used to estimate surface soil moisture over a watershed (Makkeasorn et al., 2006), oil spill boundaries on water (Topouzelis, 2008), sea state, and create ice hazard maps (Zhou et al., 2007).

2.1. Evolution of Remote Sensing Sensors and Platforms From the 1970s to the 1990s

In the 1970s, passive remote sensing techniques were first developed to monitor land and surface water conditions, and many versions that have since evolved incorporate frequent improvements (Table 3). Landsat 1, also called "Earth Resources Technology Satellite" until 1975, was launched to determine the application potential and illustrates the need for repetitive environmental monitoring. The satellite was equipped with three cameras to capture images in the red, blue, and green spectra at 185 m resolution, and a multispectral scanner (MSS) that detected four separate spectral bands between 500 and 1,100 nm at 82 m resolution. Following the success of Landsat 1, Landsat 2 and Landsat 3 were launched in 1975 and 1978, respectively; Landsat 2 utilized the same sensor specifications as Landsat 1, but the spectral band of the MSS sensor on Landsat 3 was expanded to capture radiation between 10,500 and 12,400 nm. With the launch of Landsat 4 in 1982, the spectral and spatial resolution capabilities of the sensors were further improved. The return beam vidicon (RBV) camera sensor was replaced with the thematic mapper (TM) sensor, providing seven bands of 30 m resolution pixels from 450 to 2,350 nm. Landsat 5 was launched in 1985 with the same specifications, and its TM sensor is still in use today, 25 years beyond its planned lifetime. The Coastal Zone Color Scanner (CZCS) was launched in 1978 as a proof-of-concept sensor designed to measure ocean color from space. It laid the groundwork for sensors specifically tuned to measure ocean color at a time when sensors were applied for land remote sensing and meteorological purposes. Ocean color sensors following the CZCS were the Moderate Optoelectrical Scanner (MOS), Ocean Color Temperature Scanner (OCTS), Polarization and Directionality of the Earth's Reflectances (POLDER), and Sea-Viewing Wide Field-of-view Sensor (SeaWiFS). The significant scientific accomplishments provided by data from SeaWiFS mission have been presented by Siegel et al. (2004) and McClain et al. (2004).

In 1986, the French launched SPOT 1 (Satellite Pour l'Observation de la Terre), equipped with a high resolution visible (HRV) sensor that provided 10–20 m spatial resolution pixels. Advances in spatial resolution allowed more accurate and detailed classification of targets with a 26-day revisit

TABLE 3. Evolution of remote sensing platforms from the 1970s to the 2000s

Launch date		Remote sensing platforms	Sensor (s)	Spatial resolution (m)	Band range (nm or band)	Spectral bands (# bands)	Revisit (days)
1970s	1972	Landsat 1 (ERTS 1)	RBV	185	500–750	3	18
			MSS	82	500–1100	4	
	1975	Landsat 2 (ERTS 2)	RBV	185	500–750	3	18
			MSS	82	500–1100	4	
	1978	Landsat 3	RBV	40	500–750	3	18
			MSS	82	500–12,400	5	
	1978	Nimbus 7	CZCS	825	433–12,500	6	2–3
1980s	1982	Landsat 4	MSS	82	500–1100	4	16
			TM	30–120	450–12,500	7	
	1984	Landsat 5	MSS	82	500–1100	4	16
			TM	30–120	450–12,500	7	
	1986	SPOT 1	HRV	10–20	500–890	4	26
1990s	1990	SPOT 2	HRV	10–20	500–890	4	26
	1991	ERS-1	AMI	26	C	1	35
			ATSR	1000		4	
	1992	ER-2/Twin Otter/ Proteus, and WB-57	AVRIS	20	400–2,500	224	Any Time
	1992	JERS-1	SAR	18	1275 MHZ	1	44
			OPS	18–24	OPS	18–24	
					SWIR	4	
	1993	SPOT 3	HRV	10–20	500–890	4	26
	1994	RESURS-01–3	MSU-SK	170	500–600	4	21
					600–700		
				600	700–800		
					800–1,100		
	1995	ERS-2	SAR	6–30	C	1	2–7
	1995	Radarsat 1	SAR	8–100	C	1	24
	1996	IRS P3	MOS	500	408–1600	18	2–3
	1996	ADEOS	OCTS	700	402–12,500	12	2–3
			POLDER	6,000	433–910	9	
	1997	Orbview 2	SeaWiFS	1100	402–885	8	1

	1998	SPOT 4	HRVIR	10–20	500–1,750	5	26
			Veg.	1000	430–1,750	4	
	1998	NOAA	AVHRR	500–1000	580–12,500	6	1
	1999	Landsat 7	ETM+	15–60	450–12,500	8	16
	1999	Ikonos 2	OSA	1–4	450–900	5	1.5–3
	1999	Terra (EOS AM-1)	MODIS	250–1000	405–14,385	36	1
			ASTER	520–11,650	15–90	15	
	1999	KITSAT-3 (Korea Institute of Technology Satellite-3)	CCD	15	Red, Green, Near Infrared	3	67
				15		1	
	1999	CBERS (China–Brazil Earth Resources Satellite)	WFI	260	660	2	26
					830		
			CCD	20	510–730	5	
					450–520		
					520–590		
					630–690		
					700–890		
			IR-MSS	160	500–1,100	4	
					1,550–1,750		
					2,080–2,350		
					1,040–1,250		
2000s	2000	EROS-1		1.8	500–900	1	1–4
	2000	EO-1	ALI	30	400–2,400	10	16
			Hyperion	30	400–2,400	220	
			AC	250	900–1,600	256	
	2001	Quickbird 2	PAN	0.61–2.44	445–900	5	1–3.5
	2001	PROBA	CHRIS	17 or 34	400–1,050	18 or 63	1
	2002	SPOT 5	HRS	2.5	510–730	1	26
			Veg.	1000	430–1,750	4	
			HRG	5–20	500–1,750	5	

(Continued on next page)

TABLE 3. Evolution of remote sensing platforms from the 1970s to the 2000s *(Continued)*

Launch date	Remote sensing platforms	Sensor (s)	Spatial resolution (m)	Band range (nm or band)	Spectral bands (# bands)	Revisit (days)
2002	Aqua (EOS PM-1)	MODIS	250–1000	405–14,385	36	1
2002	Envisat	MERIS	300–2360	390–1,040	15	3
2006	ALOS	PALSAR	10–100	L	1	46
2007	TerraSAR-X	SAR	1–18	X	1	2.95
2007	Radarsat 2	SAR	3–100	C	1	12–24
2007	Worldview 1	—	0.5	400–900	1	1.7–4.5
2009	Worldview 2	HRV	0.5–1.84	400–1040	9	1.1–3.7
2013	Landsat 8	OLI	15–30	433–2,300	9	16
		TIRS	100	10,300–12,500	2	

time. By 1993, SPOT 3 was in orbit but with the same 26-day revisit time. IKONOS, the first remote sensing satellite launched by a private entity, was launched in 1999 with a spatial resolution of 1 m and a revisit time of 1.5–3 days. Launched in the U.S during the same year were Landsat 7 and Terra with Moderate Resolution Imaging Spectroradiometer (MODIS) and *Advanced Spaceborne Thermal Emission and Reflection* Radiometer (ASTER) sensors. Terra provides daily near-real-time images with relatively coarse spatial resolutions (250–1,000 m) around the globe; Landsat 7 provides images with spatial resolutions (15–60 m) but low temporal resolution (16 days). In the 1990s, Japan (JERS-1), Europe (ERS-1 and ERS-2), and Canada (Radarsat-1) launched a series of satellites with SAR sensors that capitalized on microwaves to provide microwave sensing capacity with higher resolution regardless of the weather conditions (Table 3). In addition, the Airborne Visible InfraRed Imaging Spectrometer (AVIRIS) became available from an airborne sensor through the Jet Propulsion Laboratory (JPL) at the National Aeronautics and Space Administration (NASA) in 1992. The AVIRIS has a unique optical sensor that delivers calibrated images of the upwelling spectral radiance in 224 contiguous spectral bands with wavelengths from 400 to 2,500 nm with 20 m spatial resolution.

2.2. Satellite Sensors and Platforms in the Early 21st Century

Technological advances in the late 20th century led to improved satellite sensor capabilities such as finer spatiotemporal and spectral resolutions. Short revisit times of sensors such as MODIS Aqua allow more satellites to be used for real-time monitoring applications. In addition, the Medium Resolution Imaging Spectrometer (MERIS) forms part of the core instrument payload of the Environmental Satellite (ENVISAT-1) in Europe to provide hyperspectral rather than multispectral remote sensing images, allowing it to acquire data over the Earth when illumination conditions are suitable. With increased spatial and spectral resolutions, hydrologic, environmental, and ecological changes simultaneously became more noticeable, and event-based monitoring has been greatly enhanced for hazard assessment. With the increasing trend in spectral resolution, substances are more accurately classified when comparing band values. As the importance of microwave remote sensing gained recognition, satellites from Japan (ALOS), Canada (Radarsat-2), and Germany (TerraSAR-X) continued the advancement in SAR remote sensing with varying polarization (HH+HV+VH+VV) modes. At the same time, satellites managed by the United States, such as Quickbird 2, Worldview 1, and Worldview 2, provided remotely sensed optical data more often with enhanced spatial and spectral details. The upcoming launches of the Sentinel satellites in 2013–2015 will ensure continued land, ocean, and atmospheric monitoring as current sensors and platforms fail and reach the end of their life time.

TABLE 4. Summary of radiometric and geometric errors in image restoration

	External error	Internal error
Radiometric error	-Topographic attenuation -Atmospheric attenuation	-Striping -Partially missing lines
Geometric error	-Changes in platform altitude and attitude -Variations in topographic elevation	-Rotation of the Earth -Platform velocity -Panoramic distortion -Scan skew

3. IMAGE RESTORATION IN DIGITAL IMAGE PROCESSING

The sensors used to acquire remotely sensed imagery of the earth's surface are a significant distance away, which leads to distortion and modification in the electromagnetic waves emanating from the surface that must be corrected. Absorption and scattering of radiation by atmospheric particles as well as by perturbations in the sensor's platform are classified as external errors in the image data; internal errors are specifically attributed to the sensor itself. During the conversion of electromagnetic waves to digital numbers, the sensor's optical, electrical, and mechanical components may reduce data accuracy. The degree of image degradation is a function of sensor calibration and conversion efficiency. The correction of noise, distortion, and degradation inherent during image acquisition is known as image restoration. The goal is to restore the image to accurately represent conditions on the Earth's surface, thus, ensuring the highest possible data quality prior to analysis. The two main categories of error in image restoration are radiometric error and geometric error (Table 4), detailed in subsequent sections.

3.1. Radiometric Correction

3.1.1. Internal Radiometric Error

Internal radiometric errors stem from malfunctioning or improperly calibrated sensors. Striping, a form of radiometric error denoted by visible stripes on an image, can be remediated through the use of onboard lookup tables detailing radiometric values at corresponding brightness values, sensor calibration, or histogram matching. Partially missing lines or line drop out is caused during failure in data transmission, scanning equipment errors, or during image reproduction. One method for filling in a missing line is to interpolate data from nearby scan lines; another is to interpolate based on data from the same scan line at different wavelengths.

3.1.2. External Radiometric Error

Topographic and atmospheric attenuation are types of external radiometric error. Topographic error results from terrain effects and sun angle and illumination. Sloped terrain shadows areas of interest and reflects light at varying intensities. Slope–aspect correction is used to eliminate differences in illumination between two objects sharing similar reflectances and different slopes and aspects. Shadows in the terrain and diurnal or seasonal variations in illumination are caused by the changing angle of the sun in relation to the ground surface. These topographic errors originating from the sun's angle are corrected by dividing the digital number or pixel value by the sign of the solar elevation angle (the angle between the sun and the horizon).

The need for atmospheric correction for imagery from remote sensing platforms at high altitudes received attention as early as the 1970s (Austin, 1974; Clarke and Ewing, 1974; Gordon 1978, 1980; Gordon and Clark, 1980). The objective of atmospheric correction is to determine the surface reflectance from remotely sensed data by compensating for atmospheric interference. The shorter wavelengths in the electromagnetic spectrum experience greater absorption and Rayleigh scattering by atmospheric particles, making them less reliable for remote sensing purposes. The later portion of the visible region of the electromagnetic spectrum is composed of green, red, and near infrared wavelengths (520–900 nm) capable of passing through the atmosphere with reduced attenuation. Consequently, the reduced atmospheric contamination experienced by these wavelengths enhances their reliability for remote monitoring applications. In comparing false color images with and without atmospheric corrections, a visible haze overlays the image affected by atmospheric perturbations, while the color of the corrected image appears crisper.

A variety of approaches have been developed for removing atmospheric effects from remotely sensed imagery. Primary methods for atmospheric correction are as follows:

- Imaged-based methods
  - Histogram minimum method: a histogram of pixel values from all bands is assessed for low reflectance values in the visible and near infrared. The minimum values are subtracted from the surface reflectance band data because these values approximate the atmospheric contamination affecting the image (Chavez, 1988).
  - Regression method: near-zero reflectance values observed in dark pixel areas in the near-infrared image are plotted against other bands to generate a least square line fit computed using regression techniques. The corresponding offset is equivalent to the atmospheric interference, and the offset value is subtracted from the image.
- Radiative transfer models: data on atmospheric conditions at the time of image acquisition are supplied to models to compute the atmospheric path radiance. Common radiative transfer models are ATCOR, ATREM, LOWTRAN 7, MODTRAN 4, and 6S. Algorithms for specific ocean color sensors are provided in the following references:

  - GLI: Fukushima et al., 1998
  - MODIS: Gordon and Wang, 1994
  - MERIS: Antoine and Morel, 1998
  - OCTS: Fukushima et al., 1998
  - SeaWiFS: Gordon and Wang, 1994
- Empirical line method: in situ surface reflectance measurements are used to factor out atmospheric effects (Conel et al., 1987).

3.2. Geometric Correction

To generate accurate planimetric maps using remotely sensed data, geometric corrections must first be performed on the image's spatial properties to account for geometric distortions. Geometric corrections compensate for the effects of systematic and random errors, increasing the verity of individual pixel locations. These corrections are needed to obtain accurate distance, area, or direction information from images.

3.2.1. Internal and Systematic Geometric Error

Internal geometric errors are often systematic in nature and can be caused by the sensor and platform or the interaction between the remote sensing system with Earth's rotation and curvature. Correcting these errors or distortions is possible using available data about platform ephemeris, which comprise a tabular dataset detailing the location and geometric characteristics of Earth and satellite sensor during image retrieval. Specific sources of internal geometric error include the following:

- Rotation of Earth: the swatch of ground shifts during observation, leading to along-track distortion.
- Platform velocity: variations in the platform's speed generate gaps or overlap in the scanned ground track. One example would be an aircraft slowing down, leading to a greater amount of overlap than observed in the preceding scans.
- Panoramic distortion: tangential scale distortion caused by the scanning system.
- Scan skew: forward movement of the platform during scanning leads to cross-track distortion of the ground swath.

3.2.2. External and Nonsystematic Geometric Error

External geometric errors are nonsystematic errors caused by variations in the distance between the platform and Earth due to, for example, vertical topographical changes in the earth's surface. The sensor platform creates these errors as above ground level altitude varies. As altitude increases the image scale is made smaller, and as altitude decreases the image scale is made larger. In addition, geometric modifications to the image are induced by changes to the platform's attitude. One type of attitude change is roll, when the platform rotates around an axis central to the fuselage, such as when the wings on an aircraft move up or down, causing geometric distortions known as compression and expansion. For example, if the wing on the left of the aircraft drops, then image compression is experienced on all imagery to the left of the aircraft while expansion is observed to the right. Another type of attitude change experienced by a platform is pitch, when the nose or tail of the aircraft rotates upward or downward. Downward rotation of the nose compresses pixels in the front, while expanding pixels toward the aft of the fuselage. The last type of change in attitude is yaw, when the airplane rotates around the vertical or z-axis, which can displace the data by a substantial amount. Platforms can experience all possible combinations of altitude and attitude changes at a given time.

Correcting external errors requires ground control points (GCP), points on the earth's surface with available map coordinates (x and y data, degrees of longitude and latitude or distances in certain coordinate systems and projections) as well as image coordinates (row and column). Consequently, two common methods for geometric correction are image-to-map rectification and image-to-image rectification. Image-to-map rectification matches GCP between the observed image and an accurate map. Accurate maps may include hard-copy planimetric maps, digital planimetric maps, geometrically rectified digital orthophotoquads, and global positioning instruments. Image-to-image rectification translates and rotates the observed image to match another image of the same ground region. This technique may be applied when pixels do not require map projection coordinates.

4. INVERSION METHODS AND RETRIEVAL ALGORITHMS

One challenge in water quality monitoring by remote sensing is selecting a suitable inversion method to find strong relationships between water quality parameters and remotely sensed data. These methods for general calibration and image-processing methods were classified into three categories: empirical, analytical, and semi-empirical/semi-analytical (i.e., hybrid) methods. Empirical methods help determine the statistical relationships between measured water quality parameters and spectral values (Dekker et al., 1996; Yu, 2005). This method involves linear and multilinear statistical regression, curve fitting, and nonlinear regression with computational intelligence techniques such as artificial neural network (ANN), support vector machine (SVM), particle swarm optimization (PSO), and genetic programming (GP) models. Analytical methods apply the inherent optical properties (i.e., the absorption coefficient, the scattering coefficient, and the volume scattering function) and the apparent optical properties (i.e., the diffuse attenuation coefficient for downwelling irradiance and irradiance reflectance) to model the reflectance and vice versa (Dekker et al., 1996). Analytical methods for information retrieval in environmental systems emphasize analytical models, such as radiative transfer models, for processing remote sensing observations. While analytical methods are based on optical theory in physics, semi-empirical/semi-analytical methods imply the integration of empirical and analytical methods for general calibration and image-processing procedures (Ma and Dai, 2005). These hybrid methods may be expressed as empirical equations in which the optical theory in physics can be embedded (i.e., semi-empirical method) or radiative transfer theory can be expressed in an empirical way (i.e., semi-analytical method) by using regression methods to improve the overall estimation accuracy or coverage.

4.1. Empirical Methods

The common challenges of empirical methods are to find relationships between water quality parameters and spectral values (individual band, combinations of bands, or ratio of bands) by means of regression-related efforts. Traditional statistical techniques provide linear or multiple linear regressions between measured water quality parameters and remotely sensed data (Chang et al., 2009). In multiple linear regressions, the measured water quality parameters are considered as dependent variables, while spectral values from different bands are considered as independent variables. Performing multitemporal change detection with remotely sensed data via the multiple linear regressions can improve the potential of water quality monitoring. The results of linear regression models are not reliable in water bodies with high or low concentrations of water quality parameters, however, such as shallow coastal areas or inland water bodies, respectively (Chang et al., 2012; Liu et al., 2003). The presence of a nonlinear relationship among water quality parameters and the inability of linear regression methods to identify the precise relationships led scientists to develop new approaches (Wang et al., 2010); therefore, some computational intelligence models such as ANN, SVM, PSO, and GP, and their combination with other models have been applied to retrieve water quality parameters from different bands of remotely sensed data (Table 5). Empirical models developed for a specific water body may not be wholly transferable to other water bodies; however, a major advantage is that they integrate unique characteristics of the water body into the resulting model and, consequently, typically yield higher explanatory power in determining water quality conditions than a general analytical model. This advantage also poses an apparent limitation, however, because the accuracy of the empirical model may degrade when applied to surface waters with different types of chemical constituents in different environments. Thus, empirical algorithms work best when applied to the site where sampling data were collected and the formulas were derived (Liu et al., 2003; Reif, 2011),

TABLE 5. Selected empirical and hybrid methods applied to retrieve water quality parameters from remotely sensed data

Remote sensing platforms	Location	Method	Reference
ADEOS/OCTS[a]	South of Honshu, Sea of Japan, Tokyo Bay, Sagami Bay, Japan	Statistical Regression	Kishino et al. (1998)
Landsat TM	Delaware Bay, U.S.A.	Artificial Neural Network	Keiner and Yan (1998)
SPOT	Yeong-Her-Shan Reservoir, China	Genetic Programming	Chen (2003)
Landsat TM	Beaver Lake, U.S.A.	Radial Basis Function Neural Network Models (RBFN)	Panda et al. (2004)
Landsat TM	Beaver Reservoir, U.S.A.	Artificial Neural Network	Sudheer et al. (2006)
Landsat TM	Poyang Lake, China	Statistical Regression and Artificial Neural Network	Wang et al. (2008)
Landsat 7 ETM	Feitsui Reservoir, Taiwan	Incorporating Grammatical Evolution in Genetic Algorithm (GEGA)	Chen et al. (2008)
MODIS	Lake Okeechobee, U.S.A.	Genetic Programming, Artificial Neural Network, and Multiple Linear Regression	Chang et al. (2009)
Landsat TM	Taihu Lake, China	Fusion Method (Choquet Fuzzy Integral-CFI)	Wang et al. (2010)
MERIS VIS/NIR	Baltic Sea	Artificial Neural Network	Riha and Krawczyk (2011)
Landsat TM	Kissimmee River, U.S.A.	Artificial Neural Network	Chebud et al. (2012)
FieldSpec FR spectroradiometer	Shitoukoumen Reservoir, China	Genetic Algorithms and Partial Least Square (GA-PLS)	Song et al. (2012)

[a]Advanced Earth Observing Satellite/Ocean Color and Temperature Scanner.

which makes empirical algorithms useful for monitoring local water bodies for municipalities, but analytical or semi-empirical models are typically more suited for cases intended to be transferable between lakes, reservoirs, or coastal regions to address varying water quality conditions (Ma et al., 2006).

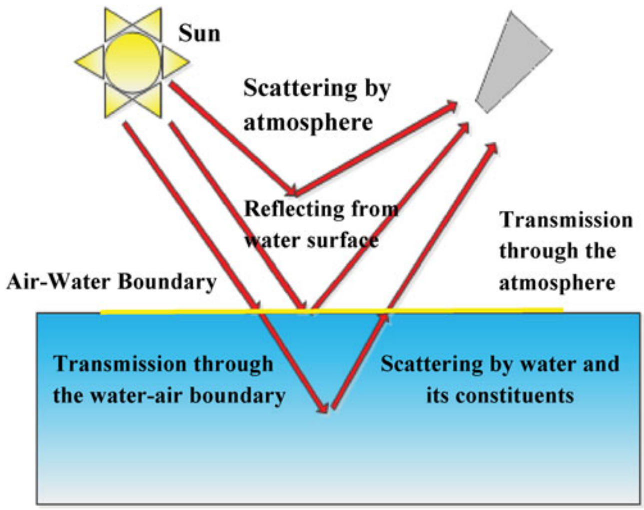

FIGURE 3. Reflectance measurement (adapted from Liew, n.d.).

4.2. Analytical Methods

Because the application of empirical methods is limited to a specific region where the samples were collected and the formula was derived, scientists have derived new, transferable methods. in which the analytical methods are developed based on optical properties correlated with the radiative transfer equation (Ma et al. 2006). Retrieval of water quality parameters in the analytical approach was based on a bio-optical approach (Yu, 2005). Bio-optical models determine the relationship between the inherent and apparent optical properties of the specific water quality parameter and the remotely sensed water reflectance. Dissolved and particulate substances cause light to scatter and attenuate after it penetrates the water surface. With such impacts induced by dissolved and particulate substances, two different parameters including inherent properties (i.e., total absorption coefficient, total scattering coefficient, and attenuation coefficient) and apparent optical properties (i.e., partial attenuation coefficient and irradiance reflectance) describe the underwater light field (Jaquet et al., 1994). The light signal leaves the water surface and reaches a sensor, carrying the inherent optical information of the water body (Figure 3). Light backscattering sends downwelling photons upward to leave the water surface. As photons leave the water surface, they affect the air–water boundary by reflectance; however, light absorption changes photons into heat or chemical energy (Tzortziou et al., 2007). Tzortziou (2007) presented the following equation for estimating remote sensing reflectance based on the backscattering and absorption:

$$R_{rs}(\lambda) = \frac{f(\lambda)}{Q(\lambda)} \cdot \frac{t_{(w,a)} t_{(a,w)}}{n_w^2} \cdot \frac{b_b(\lambda)}{a(\lambda) + b_b(\lambda)} \tag{1}$$

TABLE 6. Selected analytical methods applied for information retrieval of water quality parameters

Remote sensing platforms	Location	Method	Reference
Compact Spectrographic Imager (CASI)	Lake Braassem, the Netherlands	MIM	Hoogenboom et al. (1998)
CZCS	Mediterranean Sea	Purely Analytical Method	Ahn, 1999
MOS (Phase-I) SeaWiFS (Phase II)	North Sea	Analytical Inversion of an Optical Model	Van Der Woerd et al. (2000)
Landsat 5 TM and SPOT-HRV	Southern Frisian Lakes, the Netherlands	Forward and Inverse Bio-Optical Modeling	Dekker et al. (2001)
SPOT and Landsat TM	14 Frisian Lakes, the Netherlands	Analytical Optical Modeling	Dekker et al. (2002)
EO-1 (Hyperspectral Hyperion Data)	Moreton Bay, Australia	MIM	Brando and Dekker (2003)
Landsat 7 ETM	Moreton Bay, Australia	Analytical Model of Underwater Light Climate	Phinn et al. (2005)
EO-1 (Hypespectral Hyperion Data)	Lake Garda, Italy	MIM	Giardino et al. (2007)
Airborne Visible Infrared Imaging Spectrometer (AVIRIS)	Hudson/Raritan Estuary, New Jersey, U.S.A.	Bio-Optical Model	Bagheri (2011)

where λ is the wavelength; $b_b(\lambda)$ is the total backscattering coefficient; $a(\lambda)$ is the total absorption coefficient; t(w,a) is the water–air transmission; t(a,w) is the transmission from air to water; nw is the real part of the refractive index of the water; f is the complex function of wavelength, water inherent optical properties, solar zenith angle, aerosol optical thickness, and surface roughness; and Q is the ratio of upwelling irradiance ($Eu(\lambda)$) to upwelling radiance ($Lu(\lambda)$).

A summary of selected studies related to the applications of analytical methods in remote sensing for water quality monitoring (Table 6) shows several previous studies focused on finding a relationship between inherent and optical properties. Some applied Monte Carlo simulations for the radiation transfer to calculate the optical properties of an ocean as a function of inherent optical properties (Gordon and McCluney, 1975; Kirk, 1981). Others investigated the relationship of optical properties to particulate and

TABLE 7. Selected semi-empirical or -analytical methods applied for information retrieval of water quality parameters

Remote sensing platforms	Location	Method	Reference
CASI and CESAR	Northern Vecht Lakes, the Netherlands	Semi-empirical Method	Dekker et al. (1996)
SeaWiFS	Bedform Basin, Canada	Semi-analytical Model	Ciotti et al. (1999)
Landsat TM and Simulated SeaWiFS	Gulf of Finland	Semi-empirical Algorithm	Zhang et al. (2002)
SeaWiFS	—	Semi-analytical Garver-Siegel-Maritorena (GSM) Model	Maritorena et al. (2002)
Hyperspectral Airborne Casi and HyMap	Mecklenburg Lake District, Germany	Semi-empirical Multisensor and Multitemporal Approach	Theimann and Kaufmann (2002)
SeaWiFS MODIS	South Pacific Region (Marquesas Islands)	Semi-analytical Model-Based Ocean Color Merging Approach	Maritorena and Siegel (2005)
Hyperspectral Coupled Ocean Dynamics Experiments (HyCODE)	Mid-Atlantic Bight, U.S.A.	Semi-analytical Inversion Model	Wang et al. (2005)
SeaWiFS	UK shelf seas and NE Atlantic Ocean	Semi-analytical IOP (Inherent Optical Properties) Model	Smyth et al. (2006)
ASD FieldSpec UV-VNIR	Geist and Morse Reservoirs-Indiana, U.S.A.	Semi-empirical Remote Sensing Method	Randolph et al. (2008)
MERIS, ASTER, Airborne Hyperspectral Spectrometer (AHS)	Vecht and Veluwe lakes, the Netherlands	Semi-analytical IOP	Salama et al. (2009)
MODIS	Southern Beaufort Sea	Semi-analytical Method	Matsuoka et al. (2012)
MODIS	Gulf of Gabes, Libya	Semi-empirical Method	Katlane et al. (2012)

dissolved substances in the sea and inland waters (Bukata et al., 1981; Morel and Berthon, 1989; Morel and Prieur, 1977). In addition, bio-optical models can be used to retrieve concentrations of the specific water quality parameter from their reflectance spectra by applying analytical inversion methods such as (a) matrix inversion method (MIM), (b) ratio matrix inversion, and (c) one-band algorithm for information retrieval (Liu, 2003).

Reif (2011) mentioned the following advantages of analytical methods as compared with empirical methods: (a) analytical methods can be applied to assess optical components in the water column of both deep and shallow water bodies; (b) unlike empirical methods, analytical methods are not dependent on in situ water quality data and can be applied independently; and (c) the application of analytical methods is not limited to a specific region, and they can be applied in other lakes and reservoirs with dissimilar conditions. Although the analytical method is independent of the in situ water quality data, it is dependent on optical properties of water bodies and therefore is not a universally applicable method within a wide range of spectral bands (Reif, 2011).

In addition to satellite sensors, a few hand-held spectroradiometers were used to collect local spectral properties. Both the Compact Airborne Spectrographic Imager (CASI) and the AVIRIS are air-borne remote sensing sensors mounted on aircraft for regional studies. CASI can be used for mapping biophysical properties via radiometric and geometric analysis, and AVIRIS is a premier instrument in the realm of Earth Remote Sensing. Both were applied for water quality monitoring (Ammenberg et al., 2002; Bagheri, 2011).

4.3. Semi-Analytical/Semi-Empirical Methods

Some of the latest studies related to the application of remote sensing for water quality monitoring favored semi-empirical or -analytical (i.e., bio-optical) methods over empirical methods (Randolph et al., 2008). Semi-empirical/semi-analytical methods are based on "studying the effects of inherent optical properties of optically active variables on the applied wavelengths' reflectance" (Kallio et al., 2005). In other words, this method is a combination of analytical and empirical methods discussed in previous sections. Several previous studies conducted in the last few years applied semi-analytical/semi-empirical methods in remote sensing for water quality monitoring in varying types of water bodies worldwide (Table 7), using both air- and space-borne multispectral and hyperspectral data.

4.4. Intercomparisons Among Inversion Models

A matrix developed to address the chronological trend of applying inversion methods for monitoring water quality by remote sensing (Figure 4) shows that empirical methods are well-developed along the timeline in parallel with analytical methods as semi-empirical or semi-analytical methods were implemented to promote accuracy. Application of different inversion methods for monitoring different water quality constituents can be summarized based on their chronological order (Figure 5). The diversity of different types of methods is significant in the 2000s (Figure 4). Most methods focused on retrieving

	Empirical Methods	Analytical Methods	Semi-Emirical/Semi-Analytical Methods
1990s	• Statistical Regression • ANN	• MIM • Purely Analytical Method	• Semi-analytical Method
2000s	• Statistical Regression • GP • Radial Basis Function Neural (RBFN) Network • ANN • Back-Propagation (BP)Artificial Neural Network • Parallel Grammatical Evolution and Genetic Algorithm (GEGA)	• Ratio Matrix Inversion • Forward and Inverse Bio-optical Modeling • MIM • Analytical Model of Underwater light-climate • Analytical Optical Modeling	• Semi-Empirical Algorithm • Semi-Analytical Garver-Siegel-Maritorena (GSM) Model • Semi-Analytical Model-Based Ocean Color Merging Approach • Semi-Analytical Inversion Algorithm • Semi-Analytical IOP Model • Semi-Empirical Remote Sensing Method • Modified (GSM) Semi-Analytical Inversion Model
2010s	• Fuzzy Integral Based Fusion Method • ANN • GP • Genetic Algorithm and Partial Least Square(GA-PLS)	• Bio-optical model	• Semi-Analytical Method • Semi-Empirical Method

FIGURE 4. The chronological trend of inversion methods for monitoring water quality by remote sensing.

	Empirical Methods	Analytical Methods	Semi-Emirical/Semi-Analytical Methods
1990s	• Chlorophyll-*a* • Pigment Concentration • TSS	• CDOM • Phytoplankton • Chlorophyll-*a* • Dissolved Organic Matter	• Chlorophyll-*a* • SDD • CDOM
2000s	• Chlorophyll-*a* • TSS • DO • TP • TN • Sediment • Turbidity	• TSS • Chlorophyll-*a* • CDOM • Tripton (TR) • SDD	• Cyanobacteria • SDD • Chlorophyll-*a* • Phytoplankton • CDOM • TSS
2010s	• Chlorophyll-*a* • TSS • CDOM • Phycocyanin • Turbidity • TP	• Chlorophyll-*a*	• CDOM • Turbidity • Chlorophyll-*a*

FIGURE 5. Applications of different inversion methods for monitoring differing water quality constituents.

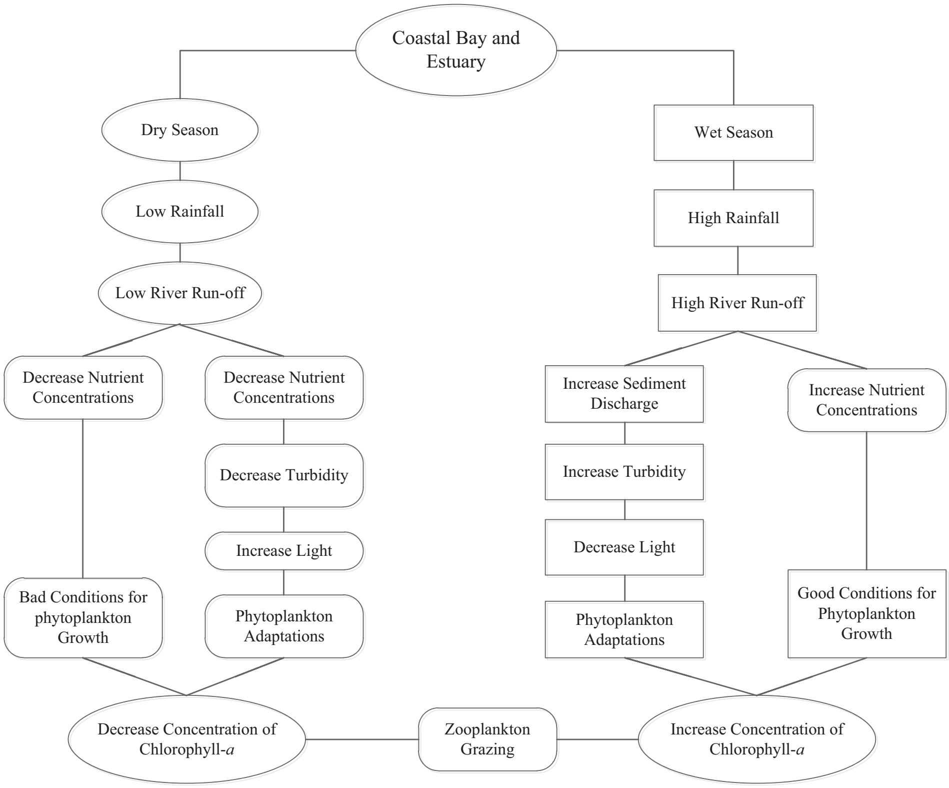

FIGURE 6. Interactions between water quality constituents and ecosystem state in response to global changes (adapted from Gilbes et al., 1996).

chlorophyll-*a* and total suspended matter (TSM). Because the accuracy of these methods is increasing, their complexity and required computational time are intricate as well.

5. APPLICATIONS OF REMOTE SENSING FOR MONITORING WATER QUALITY STATUS AND ECOSYSTEM STATE

"More than 20,000 waterbodies across America have been identified as polluted waterbodies including more than 480,000 km (300,000 miles) of rivers and shoreline and 5 million acres of lakes" (Ritchie and Cooper, n.d.). These statistics emphasize the increasing importance of water quality monitoring. For example, large variations in climatic conditions, combined with human activities and heterogeneous landscapes in coastal waters, normally produce changes in the amount and composition of river discharge (Figure 6; Gilbes et al., 1996). Changes in nutrient concentrations due to varying river discharge and their effects on phytoplankton dynamics may create a positive correlation between TSS and chlorophyll-*a* (Gilbes et al., 1996). A high TSS may imply high concentrations of nutrients, supporting amenable conditions for phytoplankton growth and resulting in high chlorophyll-*a* and TOC concentrations. With changing temperature and nutrient availability, optimum conditions for HAB may trigger the generation of high microcystin concentrations in highly eutrophied water bodies. As a result, intensive interactions between water quality constituents and ecosystem state in response to global changes frequently require advanced remote sensing to address event-driven activities and decision making.

Because conventional in situ water quality sampling limited to a local scale would be costly and labor intensive, remote sensing can increase data availability by providing two-dimensional maps derived by various inversion methods that would otherwise require a large number of in situ water quality monitoring stations. Remote sensing applications have the potential to assess the water quality of inland water bodies (lakes, reservoirs, ponds, rivers, and streams) and coastal areas (Mancino et al., 2009). In addition, screening multiple sensors and different types of inversion methods to search for the most appropriate combination can improve the retrieval accuracy of different water quality parameters. For instance, Zhang et al. (2002) showed the applicability of combined microwave and optical data to retrieve surface water quality parameters including turbidity, SDD, and TSS concentration. Zhang et al. (2004) showed the effect of considering constraint conditions on increasing the performance of ANN-based algorithms to improve retrieval accuracy for chlorophyll-*a* and CDOM. Following this study, Liu et al. (2006) presented the effect of ignoring sensor noise in spectral measurement of chlorophyll-*a* on retrieval accuracy. In addition, the inclusion of water vapor distribution can also improve the accuracy of satellite-derived sea surface temperature (SST; Emery et al., 1994; Nalli and Smith 1998; Barton, 2011). Three water constituents (algal cells, suspended solids, and CDOM) are major absorption and scattering agents within the water (Campbell et al., 2011). The applications of remote sensing for monitoring the six key water quality constituents, including TSS, chlorophyll-*a*, nutrients (TN and TP), temperature, microcystin, and TOC, to form an assessment metrics (Figure 7) will be sequentially discussed in the following sections. Each section below provides relevant historical perspectives associated with each water quality constituent of interest.

5.1. Suspended Sediment Concentrations

Suspended sediments play an important role in transporting nutrients and contaminants because a considerable amount derives from soil and bedrock erosion. The presence of suspended sediments in surface waters has negative effects on aquatic life. In addition, a high concentration of suspended sediments shortens the beneficial and efficient life of lakes and reservoirs

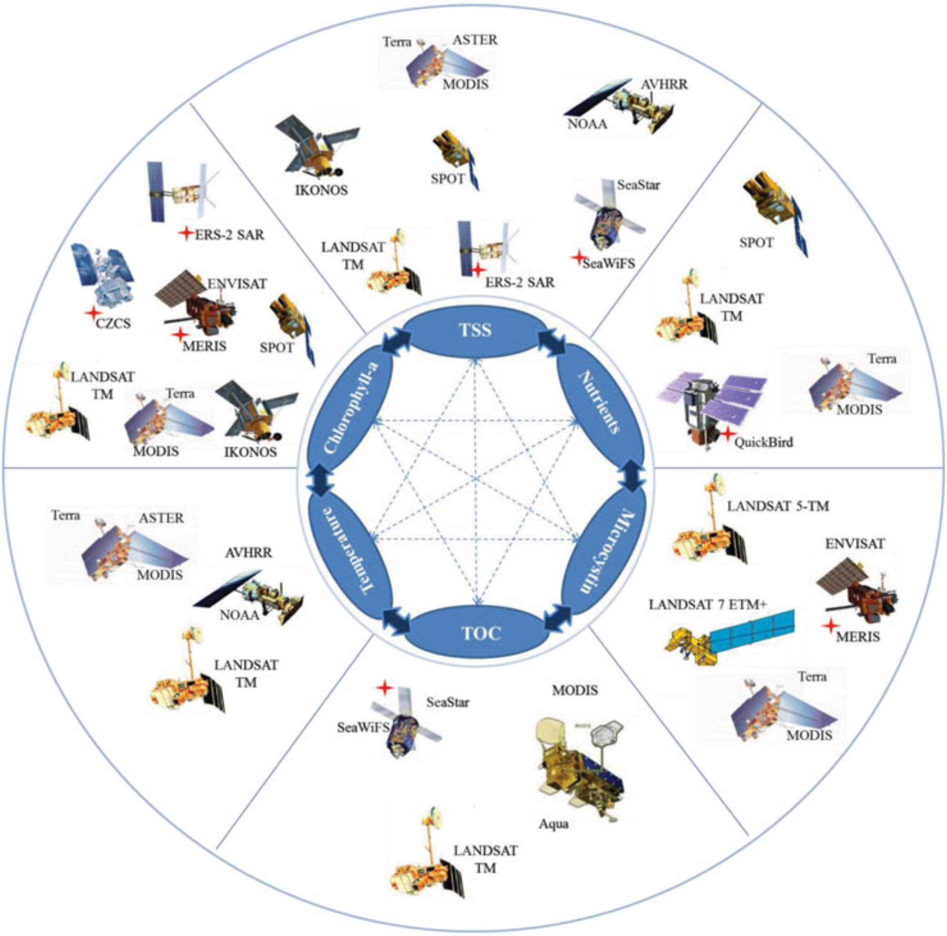

FIGURE 7. Assessment metrics and associated satellites for monitoring differing water quality constituents.
Note: Red crosses indicate satellites no longer in use.

(Lodhi et al., 1998); therefore, studying suspended sediments has become increasingly important worldwide (Bartram and Balance, 1996). Monitoring suspended sediment concentration based on in situ sampling data over large-scale water bodies is time consuming, costly, and imprecise. In such situations, remotely sensed data measured by aircraft and satellites is a promising, economical, and prompt method that can provide high spatial, spectral, and temporal resolution data.

Remote sensing of suspended sediment concentrations is based on the interaction between solar radiation with suspended sediment. Curran and Novo (1988) reviewed the relationship between suspended sediment concentrations and spectral radiance for coastal waters and showed that the surface water spectral reflectance is affected by several environmental effects such as atmosphere, sensing geometry, water–atmosphere boundary, water component, water depth, and sediment concentration.

Suspended sediment concentration has a strong relationship with reflectance from a single band or a combination of different bands (Usali and Ismail, 2010). The relationship between reflectance and suspended sediment concentration can be affected by sediment type (i.e., particle size and color), which is especially noticeable at shorter wavelengths (Novo et al., 1989). Wang et al. (2007) conducted a laboratory study to assess the relationship between different concentrations of suspended sediments with reflectance spectra and found that wavelengths in the range of b1 (430–500 nm) and b3 (670–735 nm) are best to determine lower suspended sediment concentrations, while the wavelength range of b4 (780–835 nm) is optimal for high concentration of suspended sediments, a finding confirmed by Ritchie et al. (1976), who identified an optimal wavelength range of 700–800 nm.

The empirically estimated relationships between suspended sediment concentration and reflectance, along with their correlation, were compiled for different case studies (Table 8). Ritchie et al. (1990) and Dekker et al. (2002) showed the applicability of Landsat TM4 in monitoring suspended sediment concentration in water bodies. Among the different satellites applied to monitor suspended sediment concentration, Landsat TM4 is more reliable than others.

5.2. Chlorophyll-*a* Concentrations

Chlorophyll-*a* is an important constitutent reflecting both water quality status and ecosystem state because it is required for phytoplankton existence and can be considered an indicator of algal growth or an indirect indicator of nutrients. Excessive growth of algae blooms in oceans and coastal areas decreases the amount of dissolved oxygen and causes eutrophication in rivers and streams. Because measuring chlorophyll-*a* is relatively simpler than algae biomass, chlorophyll-*a* is more often used as a trophic indicator (Huang et al., 2010). Chlorophyll-*a* measurement is costly and time consuming, but remote sensing can provide a spatial view and long term trend of this parameter. Reflectance of chlorophyll-*a* concentration varies between blue and green sections. In other words, a higher concentration of chlorophyll-*a* increases reflectance in blue wavelengths and increases the reflectance in green wavelengths (Liu et al., 2003). In addition, the atmosphere between water and sensor can affect this ratio. Dissolved organic matter (except phytoplankton) in the water as well as chlorophyll-*a c*oncentration can affect this ratio, however; radiation is highly absorbed by chlorophyll-*a* at about 450 and 670 nm (Liu et al., 2003). Jiao et al. (2006) concluded that the peak reflectance of different concentrations of chlorophyll-*a* in a lake is about 700 nm wavelength. Most empirical ocean color algorithms for determining chlorophyll-a concentration are based on the correlations between

TABLE 8. Historical applications of remote sensing for monitoring water body suspended sediment concentrations

Inversion method	Remote sensing platforms	R^2	Location	Reference
Linear Regression	Landsat	0.88	Six Northern Mississippi reservoirs, U.S.A.	Ritchie et al. (1976)
Linear Regression	Landsat MSS	0.78	Lake Chicot, Arkansas, U.S.A.	Ritchie and Schiebe (1986)
Multiple Regression		0.83		
Log-Linear Equation	Landsat TM	0.54	Delaware Bay, U.S.A.	Keiner and Yan (1998)
Neural Network		0.97		
Second Order Regression Model	Landsat 4 TM	0.99	—	Lodhi et al. (1998)
Linear Regression	AVHRR	Summer (0.94) Winter (0.024)	North Sea, Europe	Gomez (2000)
Linear Regression	CASI	0.79	The Great Miami River, Ohio, U.S.A.	Senay et al. (2001)
Regression	Landsat TM and ERS-2 SAR Data	Landsat TM (0.54), Combined Landsat TM and ERS-2 SAR (0.55)	Gulf of Finland	Zhang et al. (2002)
Neural Network		Landsat TM (0.89), Combined Landsat TM and ERS-2 SAR (0.91)		
Cubic Model (NOAA AVHRR Channel 1)	NOAA AVHRR and SeaWiFS	0.95	Louisiana Coastal and Bay, U.S.A.	Myint and Walker (2002)
Linear Model (NOAA AVHRR Channel 2)		0.9		
Power Model (SeaWiFs Channel 6)		0.85		
Multivariate	Landsat TM and ERS-2 SAR	Combined Landsat TM and ERS-2 SAR (0.578)	Gulf of Finland	Zhang et al. (2003)

(Continued on next page)

TABLE 8. Historical applications of remote sensing for monitoring water body suspended sediment concentrations *(Continued)*

Inversion method	Remote sensing platforms	R^2	Location	Reference
		Landsat TM (0.572)		
Linear Regression	Landsat TM	0.89	Lake Balaton, Central Europe	Tyler et al. (2006)
Linear Regression	IKONOS	0.83–0.97	Istanbul, Turkey	Ekercin (2007)
Linear Regression	IRS-P4	Sea (0.88)	Vedaranyam Coast in Tamilnadu, India	Ramalingam et al. (2008)
		Lagoon (0.86)		
Empirical Formula	SPOT, ASTER	0.78–0.82	The Peace-Athabasca Delta, Canada	Pavelsky and Smith (2009)
Exponential Equation	MODIS	0.73	Mayaguez Bay, Puerto Rico	Rodríguez-Guzmán and Gilbes-Santaella (2009)
Regression	ALOS	0.77	Indus River, Pakistan	Bhatti et al. (2011)
	ASTER	0.81		
Exponential Regression	MODIS	0.82	Hangzhou Bay, China	Wang et al. (2012)

chlorophyll-a concentration and spectral blue-to-green upward spectral radiance. Maximum absorption of chlorophyll-*a* occurs in the blue waveband located in the maximum phytoplankton absorption (~440 nm); however, the minimum phytoplankton absorption (~550–555 nm) occurs in the green waveband (Cannizzarro and Carder, 2006). Uncertainties may occur in determining chlorophyll-*a* concentration during cyanobacteria blooms (Usali and Ismail, 2010) or in monitoring surface water with high suspended sediment concentration (Ritchie et al., 1990). In eithor case above, the conventional blue-green ratio is less applicable because the blue light signal decreases with increasing chlorophyll-*a* concentration. The fluorescence signal will be more efficient in eutrophic waters for monitoring chlorophyll-*a* concentration, however, because (a) chlorophyll-*a* has a dominant spectral signature, (b) simple atmospheric correction is not required, and (c) fluorescence increases with intensifying chlorophyll-*a* concentration (Xing et al., 2007).

Lapucci et al. (2012) further compared Standard Ocean Color algorithms such as OC3M and MedOC3, applicable to MODIS imagery, against two new algorithms (OC5 and SAM_LT) that make use of more spectral information in MODIS data. The four algorithms perform differently in Case 1 and Case 2 waters. In general, OC3M and MedOC3 are overestimated in Case 2 waters, but the two new algorithms are less sensitive to this problem.

Hyperspectral remote sensing is more reliable for monitoring chlorophyll-*a* concentration than multispectral remote sensing because it can consider the reflectance of the extremely narrow wavebands (Jiao et al., 2006), and therefore has high potential to monitor chlorophyll-*a* concentration in water bodies (Usali and Ismail, 2010; Table 9).

5.3. Nutrients

Nutrients are considered an important parameter in water quality monitoring because they play a crucial role in algal growth, thereby affecting chlorophyll-*a* concentrations. Two representative nutrients essential for algae bloom are N and P, which limit phytoplankton growth, accelerate algae bloom, and cause eutrophication in lakes and reservoirs (Savage et al., 2010). Nutrient management issues were introduced as an important national problem by the 1997 clean water action plan of the U.S. Environmental Protection Agency (Minnesota Pollution Control Agency, 2008). The health of water bodies depends on nutrients; however, excess nutrients lead to direct and indirect responses in terms of ecosystem integrity. Direct responses include changes in chlorophyll-*a* concentration, ratio of nitrogen to phosphorous, algae bloom, and sedimentation of organic matter (Anderson, 2012); indirect responses include changes in water transparency and production of submerged aquatic vegetation as a result of varying nutrient concentrations (Anderson, 2012).

Remote sensing technologies can be used to indirectly estimate spatial and temporal distributions of N and P concentrations; however, estimating their actual concentrations is challenging because determining a direct correlation between nutrients concentrations and remote sensing spectral characteristics is difficult (Wu et al., 2010). Previous studies showed a strong correlation between suspended sediment concentration, chlorophyll-*a*, SDD, and CDOM with dissolved N and P in water bodies (Domagalski et al., 2007; Hanson et al., 2007; Heiskary and Wilson, 2005; Pacciaroni and Crispi, 2007); consequently, nutrient concentrations can be estimated by knowing spectral features of the water quality parameters of interest and finding their correlation with nutrients by using regression or new machine learning models (Chang et al., 2012b; Chang et al., 2013; Chen and Quan, 2012; Muslim and Jones, 2003). The application and reliability of remote sensing for monitoring nutrient concentrations in water bodies (Table 10) indicate that when moving into coastal bays and seas, the complexity of water quality constituents lowers the potential reliability and repeatability of retrieval models (Chang et al., 2012b; Chang et al., 2013). Both Landsat-5 TM and MODIS have been

TABLE 9. Historical applications of remote sensing for monitoring water body chlorophyll-*a* concentrations.

Inversion method	Remote sensing platforms	R^2	RMSE	Location	Reference
Regression	Landsat 4 TM	0.62–0.86	6.197–11.438	San Francisco Bay, U.S.A.	Catts et al. (1985)
Regression	Landsat TM	0.53	—	Moon Lake, Mississippi, U.S.A.	Ritchie et al. (1990)
Semi-analytical	CZCS	0.84	—	California, U.S.A.	Carder et al. (1991)
Linear Regression	Landsat TM	0.92	—	Lake Kinneret, Israel	Yacobi et al. (1995)
Regression Model	SPOT	0.95	—	Te-Chi Reservoir, Taiwan	Yang et al. (1999)
Semi-analytical (Bio-Optical Model)	MODIS	—	0.38–0.5	Gulf of Mexico and Arabian Sea	Carder et al. (1999)
Regression (Polynomial Model)	Landsat TM	0.84	—	Bull Shoals Reservoir, Arkansas, U.S.A.	Allee and Johnson (1999)
Linear Regression	CASI	0.74	—	The Great Miami River, Ohio, U.S.A.	Senay et al. (2001)
Regression	Airborne Imaging Spectrometer for Different Applications (AISA)	0.94	—	11 lakes, southern Finland	Pulliainen et al. (2001)
Linear Regression	Landsat TM	0.99	0.054	Subalpine Lake Iseo Italy	Giardino et al. (2001)
Two-Band Ratio Equation	Airborne Imaging Spectrometer for Different Applications (AISA)	0.72–0.89	0.71–1.11	A group of lakes in Finland	Kallio et al. (2001)
Regression	Coastal Zone Color Scanner (CZCS)	0.81	0.195	Black Sea	Kopelevich et al. (2002)

Neural Network		TM+ SAR (0.67) TM (0.90) TM+ SAR (0.92)		TM+ SAR (0.96) TM (0.53) TM+ SAR (0.47)			
Linear Regression	Landsat TM	0.88		—		A group of Minnesota lakes, U.S.A.	Brezonik et al. (2005)
Semi-analytical Model	Lambertian "Graycard" Reflector	—		0.172		West Florida Shelf and Grand Bahamas Bank	Cannizzaro and Carder (2006)
Semi-analytical Reflectance Model and Hyper-Spectral Approach	MODIS-aqua, SeaWiFs, MERIS	0.917		0.2185		—	Morel et al. (2007)
Linear Regression	IKONOS	0.88–0.99	—	—	—	Istanbul, Turkey	Ekercin (2007)
Linear Regression	Landsat 7 ETM	0.82	—	—	—	West lake, China	Torbick et al. (2008)
Linear Multiple Regression (LMR)	Landsat TM	0.82	3.31	0.37	—	Feitsui Reservoir, Taiwan	Chen et al. (2008)
Grammatical Evolution + Genetic Algorithm (GEGA)		0.89	2.17	0.30	—		
Two-Band and Three-Band Models	MODIS	0.58	—	—	—	Lake Malawi	Chavula et al. (2009)

(Continued on next page)

TABLE 9. Historical applications of remote sensing for monitoring water body chlorophyll-*a* concentrations.*(Continued)*

Inversion method	Remote sensing platforms	R^2		RMSE		Location	Reference
Single Band Regression	SVC HR-1024 Spectroradiometer	0.71	—	—	26.3%	Tangxun Lake, China	Huang et al. (2010)
First Derivative Regression		0.86	—	—	11.2%		
Reflectance Ratio Regression		0.86	—	—	13.8%		
Analytical model	MERIS	0.92	—	—	—	Burdekin Falls reservoir, Australia	Campbell et al. (2011)
Single Band Regression	CHRIS and MERIS	0.99	—	—	—	Group for Mediterranean Lakes	Gomez et al. (2011)
Two-Band Regression	MERIS	0.92–0.93		3.79–20.86		Group of Lakes in Eastern China	Duan et al. (2010)
Two-Band or Three-Band Models	Airborne Imaging Spectrometer for Different Applications (AISA)	0.83–0.98		5.54		Fremont Lakes, Nebraska, U.S.A.	Moses et al. (2012)
Genetic Programming	MODIS	0.72		2.9		Lake Okeechobee, Florida, U.S.A.	Chang et al. (2012a)

TABLE 10. Historical applications of remote sensing for monitoring water body nutrients

Retrieval models	Remote sensing platforms		R^2	Mean relative error (%)	Location	Reference
Multiple Linear Regression Model	Landsat 5 TM	TM1	TP (0.316)	—	Manzala Lagoon, Egypt	Dewidar and Khedar (2001)
		TM2	TP (0.394)			
		TM3	TP (0.403)			
		TM3/1	TP (0.389)			
		TM2/1	TP (0.421), TN (0.298)			
Regression	Landsat 5 TM		TN (0.75)	TN (11)	Guanting Reservoir, Beijing, China	He et al. (2008)
			TP (0.613)	TP (30)		
Linear Regression	MODIS		TP (0.56)	—	Lake Kemp, Texas, U.S.A.	El-Masri and Rahman (2008)
Multiple Regression	Landsat-5 TM + SPOT-Pan, IRS-1C/D LISS+ Pan, and Landsat-5 TM		TN (0.835)	—	Kucukcek Lake, Turkey	Alparslan et al. (2009)
			TP (0.788)			
Linear Regression	QuickBird		TN (0.94)	—	Koise River, Japan	He et al. (2010)
Regression	Landsat TM		TP (0.77)	6.6	Quintang River, China	Wu et al. (2010)
Regression	Landsat TM		TP (0.41)	—	Baltic Sea, Eastern part of Sweden	Anderson (2012)
Linear Regression	Landsat TM (Band 1,2,3,4)		TP (0.63)	TP (11.7)	Taihu Lake, China	Chen and Quan (2012)
			TN (0.24)	TN (35.6)		
Genetic Programming	MODIS		TN (0.75)		Tampa Bay, U.S.A.	Chang et al. (2012b)
Genetic Programming	MODIS		TP (0.58)		Tampa Bay, U.S.A.	Chang et al. (2013)

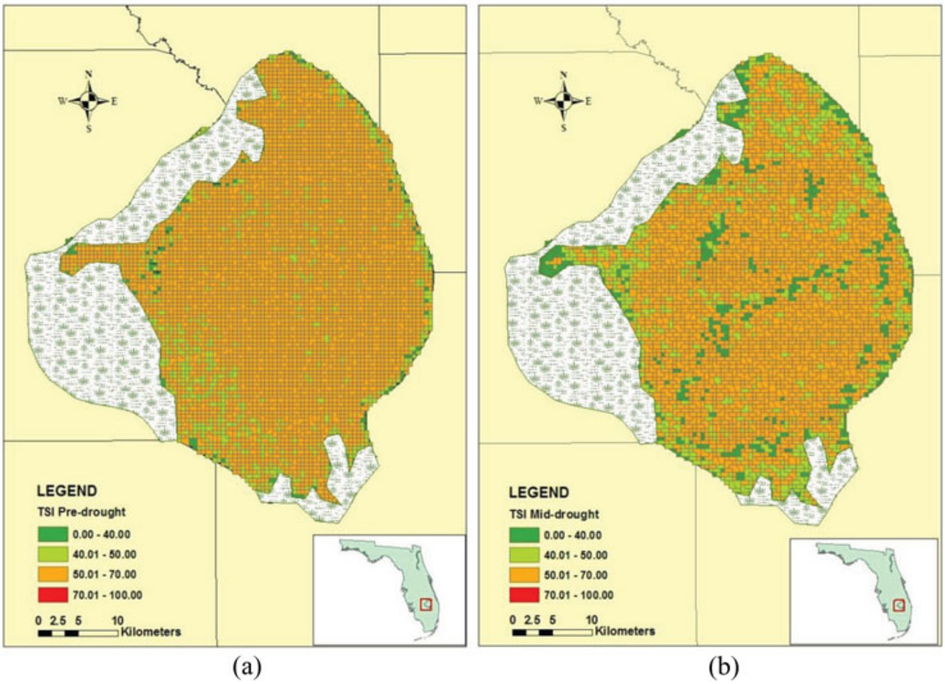

FIGURE 8. TSI estimates associated with the selected two scenarios for risk assessment and nutrient management in Lake Okeechobee, Florida (Chang and Xuan, 2012). (a) Pre-drought (August 22, 2006) (b) Mid-drought (June 11, 2007).

intensively applied for monitoring nutrients in inland water bodies (He et al., 2008; Wu et al., 2010).

The holistic assessment of lake/reservoir eutrophication can be delineated based on the Carlson's Trophic State Index (TSI) mapping (Chang and Xuan, 2012). The TSI estimates across the preselected focused scenarios show that the trophic state during the mid-drought time period is relatively lower than pre-drought conditions due to the higher TSS concentration that blocks light penetration, causing the nutrient-rich sediment to resuspend in the water column (Chang and Xuan, 2012). The use of MODIS images with a GP model generates eutrophic conditions (Figure 8). Different phytoplankton trophic indexes to assess the status of lakes can be derived using remote sensing images based on similar methods as shown in Chang and Xuan, 2012; Phillips et al., 2012).

5.4. Temperature

Water temperature is considered another important parameter of both water quality status and ecosystem state because it impacts physical, chemical, and biological reactions in water; affects the photosynthesis of aquatic plants; and controls dissolved oxygen levels in water. Monitoring surface water temperature over a wide area is costly and time consuming, and remote sensing can provide timely observations of surface water temperature over lakes, ponds, streams, and oceans; however, water temperature measurement can be influenced by different factors such as emissivity, atmospheric absorptions (e.g., water vapor, aerosols, subvisible clouds; Smith et al., 1996). Two ocean surface phenomena, evaporative and radiative cooling of the ocean surface and solar heating of the near surface layers, should be considered along with atmospheric absorption when comparing SST estimates. Barton (2011) applied three channels with central wavelengths close to 3.7, 10.8, and 12 μm to derive SST; two thermal infrared channels (11 and 12 μm) were used to retrieve SST from Advanced Very High Resolution Radiometer (AVHRR); and application of 3.7 μm data was limited to night time (Barton, 2011).

A list of satellites and techniques applied to retrieve SST was first reviewed by Barton (1995). Minnett and Barton (2010) further reviewed the status of retrieving SST from satellite measurements. The scanning radiometer (SR) on NOAA's polar orbiting weather satellite was the first infra-red satellite applied to monitor SST in the mid-1970s. The Very High Resolution Radiometer (VHRR) was then applied to provide higher resolution (eight times more than SR) on the same NOAA satellite. Later, in 1978, AVHRR, which had two infrared channels, was applied to monitor SST (Barton, 2011). In the 1990s, two other thermal infrared instruments including Along-Track Scanning Radiometer (ATSR) aboard the European Remote Sensing Satellite (ERS-2) and the Geostationary Operational Environmental Satellite (GEOS) imager were used for deriving SST. In addition, MODIS aboard NASA's earth observing systems (EOS) Terra and Aqua has been applied since 2000 and 2002, respectively. In the early 2000s, the Global Ocean Data Assimilation Experiment (GODAE) provided High Resolution SST Pilot Project (GHRSST-PP), a combination of near–real-time various SST data products including several different satellite sensors and in situ observations. To address the needs of operational models, this new generation of SST product has high spatial and temporal resolution (Donlon, 2003; Donlon et al., 2007). In addition to thermal infrared instruments, passive microwave radiometery has been applied to measure SST from remote sensing. Infrared radiometers observe the thermal radiation emitted by the sea surface in the thermal–infrared part of the spectrum; however, passive microwave radiometers indicate the emission of thermal radiation in the microwave part of spectrum (Robinson, 2004). Compared to thermal infrared SST measurement, passive microwave radiometers have less accuracy and resolution, and they are sensitive to surface roughness and precipitation but not to atmospheric and cloud effects (Maurer, 2002). Several passive microwave instruments were used to measure SST including the Scanning Multichannel Microwave Radiometer (SMMR) in the 1970s, the Tropical Rainfall Measuring Mission (TRMM) Microwave Imager

(TMI) in the 1990s, and the Advanced Microwave Scanning Radiometer (AMSR) in the 2000s (Maurer, 2002). The types of sensors and the accuracy of SST data produced from each sensor can be compared (Table 11) and the potential of different remote sensing platforms to estimate the temperature of surface water summarized (Table 12).

5.5. TOC

TOC is a nonspecific water quality indicator that includes particulate and dissolved organic carbon. Stramski et al. (1999) developed an algorithm to derive particulate organic carbon (POC) from satellite data. First, they found the relationships between POC concentrations and backscattering coefficients of suspended particles and then assessed the correlation between the spectral remote sensing and the total backscattering coefficients of water body. No in situ measurement technique is available to measure DOC concentration, but it can be measured by the optical properties of CDOM because this is the fraction of DOC that can absorb light in both the ultraviolet and visible ranges (Rochelle-Newall and Fisher, 2002). The correlation between DOC and CDOM is well established by earlier studies (Ferrari, 2000; Ferrari et al., 1996; Vodacek et al., 1995); however, this correlation is not generally observed in the open ocean areas or coastal areas (Coble, 2007). In these areas the highest concentration of DOC is depicted at the surface, whereas the CDOM concentration, as a result of photobleaching, is extremely low at the surface. In contrast, the highest concentration of CDOM is recorded below the eutrophic zone, while the DOC concentration is extremely low in this zone (Coble, 2007). Although complicated, understanding this variable relationship in coastal areas is still valuable for studying nearshore carbon cycling because of the remote sensing ability to capture daily and synoptic distributions and high concentration of DOC in these areas (Del Castillo, 2005). The dissolved fraction of TOC, called DOC, is a better predictor of disinfection by-product (DBPs) formation than including the POC in TOC measurements (Wallace, 2003); therefore, we further discuss the application of remote sensing in measuring DOC/TOC concentration by measuring CDOM fluorescence. The spectral peaks of CDOM were determined in more than 38 different lakes and reservoirs in a series of three different case studies (Chang et al, 2014; see Table 13). In addition, the application of remote sensing for monitoring DOC/TOC by measuring CDOM is presented for four selected case studies (Table 14).

5.6. Microcystin

The dynamic movement of HABs requires constant monitoring and forecasting because of the threat they pose to recreation seekers, commercial fishing operations, and water treatment facilities. While there is a variety of

TABLE 11. Typical sampling capabilities of different types of satellite SST sensors (Donlon et al., 2007)

Sensor type	Satellite type	Spatial resolution	Resampling interval	Absolute accuracy	Effect of cloud	Depth penetration
Infrared wide swath radiometer	Polar orbit	1–4 km, large off nadir angles reduce resolution	12 h, global	0.4–0.6 k	Fails over cloud and in the presence of atmosphere aerosol	Skin (10–20 μm)
Infrared dual-view radiometer	Polar orbit	1–2 km	3 days, global	0.2–0.3 k	Fails over cloud	Skin (10–20 μm)
Infrared Earth disc radiometer	Geostationary orbit	3–10 km, large off-nadir angles reduce resolution	30 min limited field of view	0.5–0.8 k	Fails over cloud	Skin (10–20 μm)
Microwave radiometer	Polar orbit	25–50 km	1–2 days, global	0.5–1 k	Affected by nonprecipitating cloud	Sub-skin (1–1.5 mm)

TABLE 12. Historical applications of remote sensing for monitoring water body temperature

Inversion method	Remote sensing platforms	R^2	P (%)	MAE [K]	RMSE [K]	SD [K]	Mean [K]	Location	Reference
Mapping SST with SEASAT Microwave Radiometer	SEASAT/ SMMR	—	—	—	—	0.7	0.22	Western North Pacific	Bernstein (1982)
Nonlinear Multichannel Algorithm	AVHRR	—	—	—	0.62–1.89	—	—	A diverse set of 110 marine profiles	Walton (1988)
Linear Regression	Landsat TM (band 6)	0.86	—	—	—	—	—	Moon Lake, Mississippi, U.S.A.	Ritchie et al. (1990)
Linear Regression	Airborne Thermal Infrared (TIR)	0.99	—	—	—	—	—	Riverine environment in eastern and western Oregon, U.S.A.	Torgersen et al. (2001)
Linear Regression	Landsat TM (band 6)	0.99	—	—	—	—	—	Daya Bay, Southern China	Chen et al. (2003)
Linear Regression	MODIS	0.99	—	—	—	—	—	Vanern and Vattern Lakes, Sweden	Reinart and Reinhold (2008)
Optimal Estimation (OE)	AVHRR	—	—	—	—	0.5	−0.2	SST collected on the global telecommunication system	Merchant et al. (2008)
Support Vector Machines (SVMs)	AVHRR	—	99.4	0.5	0.7	—	—	samples from globally distributed buoy	Moser and Serpico (2009)
Multiple Regression	MODIS	Daytime (0.89) Nighttime (0.94)	—	—	—	—	—	Itumbiara Hydroelectric reservoir, Central Brazil	Alcantara et al. (2010)

TABLE 13. CDOM spectral peaks as determined from case study analysis (Chang et al., 2014)

CDOM spectral peaks (nm)	Sampling locations	Sampling instrument	Source
570	25	Spectron Engineering SE-590 Spectrometer	Menken et al. (2005)
550, 571, 670, 710	8	Scanning Spectrophotometer	Arenz et al. (1996)
560, 650—700	5+	Spectron Instrument CE395 Spectroradiometer	Vertucci and Likens (1989)

cyanotoxins, microcystin is the main toxin produced by the cyanobacteria (World Health Organization, 1999; Hitzfield et al., 2000). The prediction of microcystin concentrations in a lake poses a unique problem because 95% is contained within healthy *Microcystis* cells (Jones and Orr, 1994); the toxin is not released until death or induced rupture of the cell wall. Thus, establishing a relationship between microcystin and other indicator substances present in the water, such as chlorophyll-*a* (Rinta-Kanto et al., 2009; Rogalus and Watzin, 2008; World Health Organization, 1999), is necessary to generate an accurate estimate of microcystin concentration. Because *Microcystis* is a bacterium that uses photosynthesis for energy production, high concentrations of *Microcystis* can be linked with elevated chlorophyll-*a* levels. Budd

TABLE 14. Historical applications of remote sensing for monitoring DOC/TOC by measuring CDOM fluorescence

Inversion method	Remote sensing platforms	Correlation between the modeled and measured DOC/TOC	Location	Reference
Simple Bio-Optical Model	ALI and Hyperion sensors (on an EO-1 platform)	0.58	13 Lakes in Southern Finland	Kutser et al. (2005)
Linear Regression	SeaWiFS	0.7	Mississippi River, U.S.A.	Del Castillo and Miller (2008)
Empirical Method	SeaWiFS and MODIS Aqua	MODIS (0.71), SeaWiFS (0.78)	Middle Atlantic Bight, U.S.A.	Mannino et al. (2008)
Genetic Programming	MODIS and Landsat 5 TM	0.34	Harsha Lake, Ohio, U.S.A.	Chang et al. (2012c)

et al. (2001) detected and tracked algal blooms using AVHRR and Landsat TM images to determine chlorophyll-*a* concentrations in the lake, a study that established the use of surface reflectance data to detect and track algal blooms based on chlorophyll-*a* levels. Wynne et al. (2008) expanded the depth of this study by using the surface reflectance of chlorophyll-*a* to specifically predict *Microcystis* blooms instead of algal blooms in general and discovered that *Microcystis* blooms can be distinguished from other cyanobacteria blooms through close analysis of the detected surface reflectance at 681 nm (Ganf et al., 1989). Studies by Mole et al. (1997) and Ha et al. (2011) had similar findings for chlorophyll-*a* as an indicator for microcystin in stabilized algae blooms that have reached the late exponential growth phase and stationary phase. In short, chlorophyll-*a* is a reliable indicator of microcystin for *Microcystis* HABs that are no longer at a peak exponential growth phase.

Phycocyanin is a pigment in all cyanobacteria (World Health Organization, 1999) that shares a positive correlation with microcystin levels (Rinta-Kanto et al., 2009). In the study by Vincent et al. (2004), Landsat TM images in the visible and infrared spectral bands were used to generate algorithms to predict phycocyanin concentrations with 73.8–77.4% accuracy. Thus, the surface reflectance of phycocyanin, chlorophyll-*a*, and *Microcystis* are suitable indicators for the prediction of microcystin levels in a lake. The surface reflectance curves for chlorophyll-*a* and phycocyanin in surface waters peak at 525, 625, 680, and 720 nm. The majority of the peaks and defining features are aptly captured by Landsat bands, which is why previous studies used this satellite for chlorophyll-*a* and phycocyanin monitoring. Chang et al. (2012c) developed the Integrated Data Fusion and Machine-learning (IDFM) to conduct a near real-time monitoring of spatiotemporal distributions of microcystin concentrations in Lake Erie using fused MODIS and Landsat 5 TM images (Chang and Vannah, 2013; Table 15).

6. FUTURE PERSPECTIVE

Satellite remote sensing may collectively provide rapid, synoptic, repeated physical and biogeochemical information on water quality status and ecosystem state. There is an apparent trend toward the use of higher spatial, spectral, and temporal resolution sensors. Increased spatial and spectral resolutions with shorter revisit times will certainly yield larger volumes of data. Data from multiple satellites and in situ sensor networks may be similar, yet minute differences will appear among the bands, projections, data scaling, and resolutions. To reduce user error and improve automated processing of sizeable data volumes, Geographical Information System (GIS) and image processing programs will need to evolve systematically to manage and unify data from multiple sources in preparation for classification, data fusion,

TABLE 15. Historical applications of remote sensing for monitoring water body microcystin

Inversion method	Remote sensing platforms	R^2	RMSE	SE (μg/l)	Location	Reference
Single-Band Regression	Landsat 7 ETM and Landsat 5 TM	0.74	—	0.64	Lake Erie, U.S.A.	Vincent et al. (2004)
Semi-Empirical Algorithm	Portable Spectroradiometer, Model PR-650 (Photo Research)	0.94	—	—	Lake Loosdercht, Lake Ijsselmeer, the Netherlands	Simis et al. (2005)
Semi-empirical Water-Leaving Radiance Algorithm	CASI-2	0.95	—	—	Barton Broad, United Kingdom	Hunter et al. (2008)
Univariate Regression (exponential, linear, polynomial, and power)	Airborne Imaging Spectrometer for Different Applications (AISA)	0.8	—	—	Geist Reservoir, Central Indiana, U.S.A.	Li et al. (2010)
Single-Band Regression	Hyperspectral sensor Data (CHRIS and MERIS)	0.97	12.92	—	Group for Mediterranean Lakes	Gomez et al. (2011)
Two-Band Regression	Hyperspectral Sensor Data (MERIS)	0.88—0.90	0.46—0.56	—	Group of Lakes in Eastern China	Duan et al. (2010)
Genetic Programming	Multispectral Sensor Data (Landsat TM and MODIS)	0.63	—	—	Lake Erie	Chang and Vannah (2013)
Three-Band Regression	YSI PC Fluorescence Probe (YSI 6600 XLM-SV)	0.96 (SA)	26.12 (SA)	—	Five drinking water sources in central Indiana, U.S.A. and South Australia (SA)	Song et al. (2013)
		0.88 (U.S.A.)	34.49 (U.S.A.)			

and manual inspection. In any circumstance, a consensus process that encourages development and implementation of open standards for geospatial contents and services is required. If reliability of data cannot be affirmed, substitute options must be offered to enhance data sharing. The concept of a sensor web that depends on the Sensor Web Enablement, developed by the Open Geospatial Consortium aided by a suite of web service interfaces and communication protocols abstracting from the heterogeneity of sensor communication, can improve the provision of alternatives. Data management in a worldwide sensor web, with essential support of various semantic modeling and annotation of sensor data, is an acute need. Various inversion and data processing models may need to be compared across various applications to sort out the best-fitted models for on-demand end users. The interoperability of web-based models (model web) can be in concert with the sensor web; thus, an integrated system of sensor web and model web to create innovative remote sensing and imaging technologies may be configured as a web-based service industry through common information gateways.

6.1. Data Fusion for Enhanced Surface Water Quality Monitoring

The satellites used for remote sensing pass over water bodies once per day at most. While this provides insight into water quality changes over a month's time, the diurnal variations are still unknown. Daily water quality dynamics should not be overlooked. The use of remote sensing to measure chlorophyll-*a* to determine phytoplankton biomass is a primary example and motivation for data merging. Phytoplankton is responsible for half of the carbon consumed through photosynthetic processes on a global scale. Knowledge of phytoplankton populations is critical for understanding the global carbon cycle; however, phytoplankton populations have the potential to double their biomass in a single day (Field et al., 1998), and the daily revisit time of a single satellite makes it impossible to capture these changes. The data gap is further widened by image contamination due to cloud cover, sun glint, aerosols, and interorbital path interludes. Merging data from satellites sharing similar bands is an encouraging method for overcoming these issues and providing additional insight into the natural variability of water quality constituents.

Data merging or data fusion is defined as the algorithmic combination of spectral, temporal, or spatial properties of two or more images into a composite image possessing the characteristics of the input images (Genderen and Pohl, 1994). Ultimately, the goal is to merge data from multiple remote sensing sensors and platforms to generate a database of daily, high resolution imagery. The advantages of applying data fusion to surface water remote sensing are as follows:

1. Enhanced global coverage of surface waters, yielding image products at higher spatial and temporal resolutions.

2. Data from multiple satellite sensors increase the statistical validity of the extracted water quality parameters.
3. Data are acquired from a single database with a uniform storage format and processing level instead of from multiple sensors and platforms at various processing extents, storage formats, and acquisition policies.

The benefits of data fusion for surface water remote Sensing are significant, but they rely on a collaborative effort among the various space agencies. In addition to differing political interests, platforms and sensors are often built for a specific mission or objective. If these various obstacles can be overcome, and surface water sensing is shifted from mission oriented to measurement oriented, then the goal for daily, global surface water datasets is most definitely viable.

Last, a few remaining issues must be addressed for future development of a merged dataset. As previously mentioned, the multisensor data should be readily available at no cost from a single provider. This provides a uniform dataset to end users, without necessitating detailed knowledge of the numerous data processing methods, storage formats, acquisition requirements, and data usage policies and leads to a concurrent point that has plagued existing datasets. The methods used to process raw sensor data for atmospheric, geometric, and radiometric errors and other biases have improved with time. Subsequently, entire datasets have been reprocessed in the middle of ongoing, multiyear missions. Dataset stability is difficult to address because the evolution of processing methods yields more accurate datasets. This problem is compounded by the number of sensors, which are subject to dataset adjustments. End users may find monitoring several sensors challenging, without the additional onus of understanding how each one works and how the data quality has changed over time. Changing datasets directly impact attempts to compare studies that used the same sensor but possess different qualities of data. No solution has yet been found except to freeze existing datasets for set periods of time, or unless the improvement in data quality surpasses a set threshold. Not only can processing algorithms change for each sensor, but the entire data fusion methodology must be standardized. Multiple merging techniques exist that can be applied independently or in combination. An important consideration is whether the data fusion techniques applied should be specifically calibrated for a water quality parameter, or whether a single fusion algorithm that exhibits acceptable performance for identifying multiple water quality parameters should be selected. As researchers continue to develop and improve data fusion techniques, the resulting solution to this quandary will continue to change.

6.2. Atmospheric Correction Methods

Existing atmospheric correction methods are effective in Case 1 waters, which primarily consist of open ocean waters; however, these algorithms can be further developed when processing shorter visible wavelengths, such as blue, as a result of errors caused by extrapolating the effects of aerosols. For optically complex inland water bodies, turbid coastal waters, and atmospheric conditions over surface waters plagued by heavy particulates, aerosols, and pollutants, improvements to atmospheric correction algorithms are needed to provide more accurate monitoring of water quality conditions (Wang, 2010). Once again, processing data in the blue wavelengths yields less accurate data products for Case 2 waters with high sediment contents, especially for Case 2 waters with high CDOM concentrations. In cases of aerosols exhibiting strong absorbance, a report by the International Ocean-Colour Coordinating Group (IOCCG; Wang, 2010) found that the mean error for water-leaving radiance was between –35 to –60%. The proposed solution for strongly absorbing aerosols is to properly identify the presence of the aerosols by using UV band data and mapping the vertical distribution of the aerosol between the sensor and the target site. These difficulties may require atmospheric correction algorithms to be developed or specifically calibrated for coastal zones, complex ocean waters, and regions with aerosols demonstrating strong absorbance.

6.3. Future Evolution of Inversion Models for Case 2 Waters

Case 2 waters comprise a small percentage of global surface water, but understanding the water quality conditions is paramount due to the potential for frequent human interaction and the resulting economic and ecological impacts. Coastal and inland water bodies may fluctuate between Case 1 and Case 2 states, and inversion models must be developed to interpret water quality under both conditions. Due to the optical complexity of Case 2 waters, the algorithms developed for Case 1 waters—typically simple analytical algorithms—are not suitable to interpret the nonlinear relationship between water quality parameters and surface reflectance (Shubha, 2000). Case 1 algorithms may feature band ratios using 2–3 wavelengths to determine water quality, whereas Case 2 algorithms can require several wavelengths as input to interpret conditions. Furthermore, conditions in Case 2 waters may exhibit seasonal change, which requires unique algorithms specifically calibrated for that region or water body. As a result, the empirical or semi-empirical model developed for one type of Case 2 water will not perform well when applied to another Case 2 water body with a vastly different water-leaving radiance. The development of empirical algorithms through sophisticated techniques, such as nonlinear optimization, principal component analysis, SVM, ANN, PSO, and GP, must continue to be developed and optimized for individual water quality parameters. The end goal is to apply these algorithms at a global scale, but to support this endeavor, extensive libraries cataloging measurements of inherent optical properties for all ranges of water quality conditions would need to be developed (Shubha, 2000). Lastly, uniform and standardized procedures for testing and validating the algorithms are required for proper comparison between algorithms and their results.

The IDFM technique was developed to meet this requirement of near real-time monitoring using optical sensors (Chang et al., 2012c). IDFM integrates data fusion techniques and empirical inversion models to characterize water quality in Case 1 and Case 2 waters on a near real-time basis. A case study detailing the use of this algorithm for optimizing a drinking water treatment operation in a Case 2 water body is provided. Landsat 5 TM and MODIS Terra satellite imagery can be acquired free of charge, but MODIS has coarse spatial resolution, while Landsat has a lengthy 16-day revisit time. This difficulty is solved by using data fusion algorithms to fuse the fine spatial resolution of Landsat with MODIS data of the daily repeat cycle to generate a synthetic image with both high spatial and temporal resolution. To demonstrate the capabilities of IDFM, the case study in Chang et al. (2012c) uses the fused surface reflectance band data and applied machine-learning techniques to reconstruct the spatiotemporal distribution of TOC in Harsha Lake, Ohio. Fusing MODIS data with Lansat-5 TM can promote optimal pumping at the source water intake for the McEwen Water Treatment Plant in Ohio. The use of hyperspectral remote sensing images, with the aid of more detailed analytical methods (Brando and Dekker, 2003; Campbell et al., 2011), can be inevitable when characterizing unique algal blooms and relevant species in water bodies, such as microcystin, yet this near real-time monitoring system cannot function well on cloudy days. The use of SAR, an active remote sensing system, has become increasingly popular over the last decade due to the advantages it offers over optical sensors. Because microwaves are sufficiently long to pierce through cloud cover and smoke, readings can be collected in all weather conditions, a useful feature for satellites without a sun-synchronous orbit, or those that orbit at higher latitudes. Real-time monitoring applications using IDFM will greatly benefit from the reliability that SAR introduces, and future inversion models should be improved to integrate the water-leaving radiance at these wavelengths. Remotely sensed data uninterrupted by smoke and cloud cover is crucial for the future of real-time, event-based, routine environmental monitoring.

6.4. Web-Based Decision Support

Although scientists may have a thorough understanding of remote sensing platforms, GIS processing techniques, error correction algorithms, and inversion models related to remote sensing of surface water quality, the end users who would put these methods into practice for real-world applications are not always trained or knowledgeable in these areas. Web-based decision support through a simple and streamlined interface is needed to allow decision makers access to these advancements. Web-based decision support that includes model-web and sensor-web in the next generation environmental informatics platform must be readily accessible to end users; its framework would consist of a client-based, user-friendly interface where historical or near real-time water quality information could be retrieved by entering the location of the water body and selecting the water quality parameters of interest. Concentration maps highlighting spatiotemporal distributions of parameter would allow decision makers to assess the health of marine ecosystems, discover biochemical cycles, detect harmful algal bloom formation and movement, observe ocean–atmospheric interactions, and prepare for seasonal changes common to the water body; however, this can only be made possible through multinational collaboration.

The global surface water body database for a comprehensive web-based decision support system would require continuous and sustainable coverage of the oceans and inland water bodies. Having access to a variety of interoperable sensors, data, and models, and data streamlining from ground-based to airborne, and to space-borne remote sensing sensors can be connected using sensor web. The concept of the sensor web is a type of sensor network that is especially well suited for environmental monitoring based on changing requirements allowing sensor technology, computer technology and network technology to advance together with the need in real world systems. For example, the Sensor Web Enablement (SWE) standards promoted by the Open Geospatial Consortium enable developers to make all types of sensors, transducers and sensor data repositories discoverable. The web-based decision support system for Sensor Web may use a network of sensors linked by software and the internet to an autonomous satellite observation response capability. This capacity may be expanded by model web further that could increase model interoperability and access and potentially produce a variety of end user-oriented portfolios of environmental observations. Such a new cyberinfrastructure that is community-driven, collaborative approach will enable us to further perform multisensory data fusion with the aid of sensor modeling to enlarge the integrative benefits. It is known that the Internet of Things (IoT) enables communication between smart objects promoting the pervasive presence around us of a variety of things or objects which are able to interact with each other and cooperate to reach common goals (Atzori et al., 2010). Data fusion mechanism based in the services composition model for the IoT may be the ultimate goal to weave the sensor, data, and mode fusion in the end.

The existing problem, however, is that coordinating the discrepancies among existing systems and achieving interoperability for new systems requires well-configured, next-generation informatics platforms. Even if such a new infrastructure system with interwoven sensor and model webs existed, there is no guarantee that near real-time or real-time remote sensing networks could be in place. Integrated data fusion with a wealth of imaging processing models must also meet the mission-oriented goal. Along this line, for example, The IOCCG has developed a conceptual outline to implement the aforementioned sensor–web support system, termed the International Network for Sensor InTercomparison and Uncertainty assessment for Ocean-Color Radiometry (INSITU-OCR). This network would consist of a "concerted international and interagency effort to coordinate activities relating to satellite ocean-color sensor inter-comparison and uncertainty assessment of datasets required for essential climate variable generation" (McClein and Meister, 2012). The IOCCG would manage calibration of the sensors to ensure consistency in the satellite data products, synchronize sharing and collection protocols for in situ data, coordinate and standardize algorithm development to ensure proper inter-comparison of algorithms, and manage a series of single-processing software packages that end users could access for processing and picturing data products. The facets of this monumental yet necessary undertaking would need to be extrapolated until the full web-based decision support system is attained, but once established, this system would streamline and revolutionize both the research of water quality remote sensing and its real world applications. Such improvements may lead to future exploration of the following challenges tailored for different types of end users:

1. What remote sensing platforms, sensors, and inversion modeling techniques are available, or can be developed to identify water quality changes across historical data records of extreme events that impact ecosystem states?
2. Can these platforms, sensors, and inversion modeling techniques demonstrate the linkages among observed events, past trends in events, and predicted climate change-induced extreme events that impact water quality and ecosystem integrity?
3. What platforms, sensors, and inversion modeling techniques can provide local- and regional-scale information on extreme events to policy makers and planners challenged with developing sustainable systems over the next several decades that affect drinking water quality, watershed management, and aquatic ecosystem restoration?
4. How can water quality monitoring networks be enhanced to support the numerical models to capture the changes in various kinds of extreme events that impact water quality in a real-time basis in different regions or country over the next several decades?

7. CONCLUSIONS

This analysis presents a thorough review of advancements over the past four decades in environmental remote sensing technologies for monitoring water quality status and ecosystem state in relation to nutrient cycling. Chronological trends were analyzed over the time horizon to signify the changes in both hardware and software development. Six relevant constituents and descriptors of interest were included in the assessment metrics including TSS, chlorophyll-*a*, nutrients (TN and TP), temperature, TOC, and microcystin concentrations, all of which can be systematically linked in aquatic environments based on their salient features in relation to nutrient dynamics. Future perspectives in terms of functionalities, implementations, and challenges in the nexus of environmental informatics and remote sensing involving technologies of data acquisition, communication, storage, image processing, and information retrieval were elaborated to improve the odds of success of remote sensing analyses.

Overall, remote sensing technologies involve using a wealth of multidisciplinary approaches to solve highly interdisciplinary problems and provide essential monitoring capacity for terrestrial, atmospheric, and aquatic environments. As each disciplinary area evolves, the follow-up utilization must be holistically modified by various mission-oriented programs such as Soil Moisture and Ocean Salinity (SMOS) and Soil Moisture Active Passive (SMAP), among others; nevertheless, such progress will certainly contribute to overall economic, environmental, and social benefits. The gaps between perception and decision making will be minimized with the recent development of IoT, which would include sensor and model webs as the next generation informatics platform widely available for promoting remote sensing applications.

NOMENCLATURE

Abbreviations

Acronym	Meaning
AISA	Airborne Imaging Spectrometer for different Applications
ALOS	Advanced Land Observation Satellite
ANN	Artificial Neural Network
ASTER	Advanced Spaceborne Thermal Emission and Reflection Radiometer
AVHRR	Advanced Very High Resolution Radiometer
AVIRIS	Airborne Visible/Infrared Imaging Spectrometer
CASI	Compact Airborne Spectrographic Imager
CBERS	China-Brazil Earth Resources Satellite
CDOM	Colored Dissolved Organic Matter
CERP	Comprehensive Everglades Restoration Plan
CZCS	Coastal Zone Color Scanner
DO	Dissolved Oxygen
DOC	Dissolved Organic Carbon
ENVISAT	Environmental Satellite

EO-1	Earth Observing-1
EOS	Earth Observing System
EROS	Earth Resources Observation Satellite
ERS	European Remote-Sensing Satellite
ERTS	Earth Resources Technology Satellite
ETM+	Enhanced Thematic Mapper Plus
GA-PLS	Genetic Algorithms with Partial Least Squares
GEGA	Grammatical Evolution - Genetic Algorithm
GIS	Geographical Information System
GP	Genetic Programming
HABs	Harmful Algal Blooms
HRG	High Resolution Geometric
HRV	High Resolution Visible
HRVIR	High Resolution Visible and Infrared
IDFM	Integrated Data Fusion and Machine-learning
IoT	Internet of Things
IR	Infrared
IRIS	Internet Routing in Space
IRS	Indian Remote Sensing
JPL	Jet Propulsion Laboratory
JERS-1	Japanese Earth Resources Satellite 1
KITSAT	Korea Institute of Technology Satellite
LMR	Linear Multiple Regression
MERIS	Medium Resolution Imaging Spectrometer
MIR	Mid-band Infrared
MODIS	Moderate-Resolution Imaging Spectroradiometer
MAE	Mean Absolute Error
MSS	Multispectral Scanner System
MW	Microwave
N	Nitrogen
NH3	Ammonia
NIR	Near Infrared
NOx	Nitrogen Oxides
NOAA	National Oceanic and Atmospheric Administration
NRC	National Research Council
OSA	Optical Sensor Assembly
P	Phosphorous
Pan	Panchromatic
PALSAR	Phased Array type L-band Synthetic Aperture Radar
PSO	Particle swarm Optimization
RADAR	Radio Detection and Ranging
RBFN	Radial Basis Function Network
RBV	Return Beam Vidicon
RMSE	Root Mean Square Error

SAR	Synthetic Aperture Radar
SDD	Secchi Disk Depth
SE	Standard Error
SeaWiFS	Sea-viewing Wide Field-of-view Sensor SeaWiFS
SMMR	Scanning Multi-channel Microwave Radiometer
SMAP	Soil Moisture Active Passive satellite
SMOS	Soil Moisture and Ocean Salinity satellite
SPOT	Système Pour l'Observation de la Terre
SR	Scanning Radiometer
SST	Sea Surface Temperature
SVM	Support Vector Machine
TIR	Thermal Infrared
TM	Thematic Mapper
TN	Total Nitrogen
TNDVI	Transformed Normalized Difference Vegetation index
TOC	Total Organic Carbon
TP	Total Phosphorous
TSI	Trophic State Index
TSM	Total Suspended Matter
TSS	Total Suspended Solids
USEPA	United States Environmental Protection Agency
USGS	United States Geological Survey
VHRR	Very High Resolution Radiometer
VIS	Visible
WHO	World Health Organization

REFERENCES

Ahn, Y. (1999). Development of inverse model from ocean reflectance. *Marine Technology Society Journal*, 33, 69–80.

Alcantara, E. H., Stech, J. L., Lorenzzetti, J. A., Bonnet, M. P., Casamitjana, X., Assireu, A. T., and Moraes Novo, E. M. L. (2010). Remote sensing of water surface temperature and heat flux over a tropical hydroelectric reservoir. *Remote Sensing of Environment*, 114, 2651–2665.

Allee, R. J., and Johnson, J. E. (1999). Use of satellite imagery to estimate surface chlorophyll-*a* and Secchi disc depth of Bull Shoal s Reservoir, Arkansas, USA. *International Journal of Remote Sensing*, 20, 1057–1072.

Alleman, R. (2012). *2012 South Florida Environmental Report*. West Palm Beach, FL: South Florida Water Management District.

Alparslan, E., Coskun, H. G., and Alganci, U. (2009). Water quality determination of Kucukcekmece Lake, Turkey by using multispectral satellite data. *The Scientific World Journal*, 9, 1215–1229.

Ammenberg, P., Flink, P., and Lindell, T. (2002). Bio-optical modeling combined with remote sensing to assess water quality. *International Journal of Remote Sensing*, 23, 1621–1638.

Andersson, M. (2012). *Estimating phosphorous in rivers of Central Sweden using Landsat TM data*. Research report, Stockholm University, Sweden.

Antoine, D., and Morel, A. (1998). Relative importance of multiple scattering by air molecules and aerosols in forming the atmospheric path radiance in the visible and near-infrared parts of the spectrum. *Applied Optics*, 37, 2245–2259.

Arenz, R., Lewis, W., and Saunders, J. (1996). Determination of chlorophyll and dissolved organic carbon from reflectance data for Colorado reservoirs. *International Journal of Remote Sensing*, 17, 1547–1566.

Atzori, L., Iera, A., and Morabito, G. (2010). The internet of things: A survey. *Computer Networks*, 54, 2787–2805.

Austin, R. W. (1974). The remote sensing of spectral radiance from below the ocean surface. In: Jerlov, N. G., Nielsen, E. S. (Eds.) *Optical aspects of oceanography* (pp. 317–344). San Diego, CA: Academic Press.

Bagheri, S. (2011). Nearshore water quality estimation using atmospherically corrected AVIRIS data. *Remote Sensing*, 3, 257–269.

Barton, I. J. (1995). Satellite-derived sea surface temperatures: Current status. *Journal of Geophysical Research*, 100, 8777–8790.

Barton, I. J. (2011). Improving satellite-derived sea surface temperature accuracies using water vapor profile data. *Journal of Atmospheric and Oceanic Technology*, 28, 85–93.

Bartram, J., and Balance, R. (1996). *Water quality monitoring: A practical guide to the design and implementation of freshwater quality studies and monitoring programs*. Geneva, Switzerland: United Nations Environment Program and the World Health Organization.

Bernstein, R. L. (1982). Sea surface temperature mapping with the sea SAT microwave radiometer. *Journal of Geophysical Research*, 87, 7865–7872.

Bhatti, A. M., Nasa, S., and Takagi, M. (2011). Multi spectral remotely sensed models for monitoring suspended sediment: A case study of Indus River, Pakistan. *International Journal of Water Resources and Arid Environments*, 1, 417–427.

Brando, V. E., and Dekker, A. G. (2003). Satellite hyperspectral remote sensing for estimating estuarine and ciastal water quality. *IEEE Transactions on Geoscience and Remote Sensing*, 41, 1378–1387.

Brezonik, P., Menken, K. D., and Bauer, M. (2005). Landsat-based remote sensing of Lake water quality characteristics, including chlorophyll and colored dissolved organic matter (CDOM). *Lake and Reservoir Management*, 21, 373–382.

Budd, J., Beeton, A., Stumpf, R., Culver, D., and Kerfoot, W. (2001). Satellite observations of Microcystis blooms in western Lake Erie. *Verhandlungen des Internationalen Verein Limnologie*, 27, 3787–3793.

Bukata, R. P., Bruton, J. E., Jerome, J. H., Jain, S. C., and Zwick, H. H. (1981). Optical water quality model of Lake Ontario. 2: Determination of chlorophyll-*a* and suspended mineral concentration of natural waters from submersible and low altitude optical sensors. *Applied Optics*, 20, 1696–1703.

Campbell, G., Phinn, S. R., Dekker, A. G., and Brando, V. E. (2011). Remote sensing of water quality in an Australian tropical freshwater impoundment using matrix inversion and MERIS images. *Remote Sensing of Environment*, 115, 2402–2414.

Cannizzaro, J. P., and Carder, K. L. (2006). Estimating chlorophyll-*a* concentration from remote-sensing reflectance in optically shallow waters. *Remote Sensing of Environment*, 101, 13–24.

Carder, K. L., Chen, F. R., Lee, Z. P., and Hawes, S. K. (1999). Semianalytical moderate-resolution imaging spectrometer algorithm for chlorophyll-*a* and absorption with bio-optical domains based on nitrate-depletion temperatures. *Journal of Geophysical Research*, 104, 5403–5421.

Carder, K. L., Hawes, S. K., Baker, K. A., Smith, R. C., Steward, R. G., and Mitchel, B. G. (1991). Reflectance model for quantifying chlorophyll-*a* in the presence of productivity degradation products. *Journal of Geophysical Research: Oceans*, 46, 20599–20611.

Catts, G. P., Cloern, J. E., Knight, A. W., and DeGloria, S. D. (1985). Remote sensing of tidal chlorophyll-*a* variations in estuaries. *International Journal of Remote Sensing*, 6, 1685–1706.

Chang, N. B., Daranpob, A., Yang, J., and Jin, K. R. (2009). A comparative data mining analysis for information retrieval of MODIS images: Monitoring lake turbidity changes at Lake Okeechobee, Florida. *Journal of Applied Remote Sensing*, 3, 033549.

Chang, N. B., and Hong, Y. (2012). *Multiscale hydrologic remote sensing: Perspectives and applications*. Boca Raton, FL: CRC Press.

Chang, N. B., Hossain, F., and Wanielista, M. (2010a). Use of filter media for nutrient removal in natural systems and built environments (I): Previous trends and perspectives. *Environmental Engineering Science*, 27, 689–706.

Chang, N. B., and Vannah, B. (2013). *Intercomparisons between empirical models with data fusion techniques for monitoring water quality in a large lake*. Paper presented at the IEEE International Conference on Networking, Sensing and Control (IEEE Systems, Man, and Cybernetics Society), Paris, France, April 10–12.

Chang, N. B., Vannah, B., and Xuan, Z. (2012c). *Monitoring the total organic carbon concentrations in a lake with the integrated data fusion and mining technique*. Presented at SPIE OP403: Remote Sensing and Modeling of Ecosystems for Sustainability VII Symposium at San Diego, California.

Chang, N. B., Vannah, B. W., Yang, V. Y., and Elovitz, M. (2014). Integrated data fusion and mining techniques for monitoring total organic carbon concentrations in a lake. *International Journal of Remote Sensing*, 35, 1064–1093.

Chang, N. B., Wanielista, M., and Makkeasorn, A. (2010b). Use of filter media for nutrient removal in natural systems and built environments (II): Design challenges and application potentials. *Environmental Engineering Science*, 27, 707–720.

Chang, N. B., and Xuan, Z. (2012). Chapter 2: Using remote sensing-based Carlson Index mapping to assess hurricane and drought effects on lake trophic state. In N. B. Chang (Ed.), *Environmental remote sensing and systems analysis* (pp. 7–24). Boca Raton, FL: CRC Press.

Chang, N. B., Xuan, Z. M., and Wimberly, B. (2012b). Remote sensing spatiotemporal assessment of nitrogen concentrations in Tampa Bay, Florida due to a drought. *Journal of Terrestrial, Atmospheric and Oceanic Sciences*, 23(5), 1–12.

Chang, N. B., Xuan, Z., and Yang, J. (2013). Exploring spatiotemporal patterns of phosphorus concentrations in a coastal bay with MODIS images and machine learning models. *Remote Sensing of Environment*, 134, 100–110.

Chang, N. B., Yang, J., and Daranpob, A. (2010c). Medium-term Metropolitan Water Availability Index (MWAI) assessment based on synergistic potentials of multi-sensor data. *Journal of Applied Remote Sensing*, 4, 043519.

Chang, N. B., Yang, J., Daranpob, A., Jin, K. R., and James, T. (2012a). Spatiotemporal pattern validation of chlorophyll-*a* concentrations in Lake Okeechobee, Florida using a comparative MODIS image mining approach. *International Journal of Remote Sensing*, 33, 2233–2260.

Chavez, P. S. Jr. (1988). An improved dark-object subtraction technique for atmospheric scattering correction of multispectral data. *Remote Sensing of the Environment*, 24, 459–479.

Chavula, G., Brezonik, P., Thenkabail, P., Johnson, T., and Bauer, M. (2009). Estimating chlorophyll concentration in Lake Malawi from MODIS satellite imagery. *Physics and Chemistry of the Earth*, 34, 755–760.

Chebud, Y., Naja, G. M., Rivero, R. G., and Melesse, A. M. (2012). Water quality monitoring using remote sensing and an arificial neural network. *Water, Air, and Soil Pollution*, 223, 4875–4887.

Chen, C., Shi, P., and Mao, Q. (2003). Application of remote sensing techniques for monitoring the thermal pollution of cooling-water discharge from nuclear power plant. *Journal of Environmental Science and Health, Part, A–Toxic/Hazardous Substances and Environmental Engineering*, A38, 1659–1668.

Chen, J., and Quan, W. (2012). Using Landsat/TM imagery to estimate nitrogen and phosphorous concentration in Taihu Lake, China. *IEEE Journal of Selected Topics in Applied Earth Observations and Remote Sensing*, 5, 273–280.

Chen, L. (2003). A study of applying genetic programming to reservoir trophic state evaluation using remote sensor data. *International Journal of Remote Sensing*, 24, 2265–2275.

Chen, L., Tan, C. H., Kao, S. J., and Wang, T. S. (2008). Improvement of remote sensing on water quality in a subtropical reservoir by incorporating grammatical evolution with parallel genetic algorithms into satellite imagery. *Water Research*, 42, 296–306.

Chorus, I., and Fastner, J. (2001). Recreational exposure to cyanotoxins. In: I. Chorus (Ed.), *Cyanotoxins, occurrence, causes, consequences* (pp. 190–199). Heidelberg, Germany: Springer.

Ciotti, A. M., Cullen, J. J., and Lewis, M. R. (1999). A semi-analytical model of the influence of phytoplankton community structure on the relationship between light attenuation and ocean color. *Journal of Geophysical Research*, 104, 1559–1578.

Clarke, G. L., and Ewing, G. C. (1974). Remote spectroscopy of the sea for biological production studies. In N. G. Jerlov and E. Steemann-Nielsen (Eds.), *Optical aspects of oceanography* (pp. 389–413). New York: Academic Press.

Coble, P. G. (2007). Marine optical biogeochemistry: The chemistry of ocean color. *Chemical Reviews*, 107, 402–418.

Conel, J. E., Green,R. O., Vane, G., Bruegge, C. J., and Alley, R. E. (1987). AIS-2 radiometry and a comparison of methods for the recovery of ground reflectance. In G. Vane (Ed.), *Proceedings of the 3rd Airborne Imaging Spectrometer Data Analysis Workshop* (pp. 18–47). Pasadena, CA: Jet Propulsion Laboratory.

Curran, P. J., and Novo, E. M. M. (1988). The relationship between suspended concentration and remotely sensed spectral radiance: A review. *Journal of Coastal Research*, 4, 351–368.

Dekker, A. G., Vos, R. J., and Peters, S. W. M. (2001). Comparison of remote sensing data, model results and in situ for total suspended matter (TSM) in the Southern Frisian lakes. *Science of the Total Environment*, 268, 197–214.

Dekker, A. G., Vos, R. J., and Peters, S. W. M. (2002). Analytical algorithms for lake water TSM estimation for retrospective analysis of TM and SPOT sensor data. *International Journal of Remote Sensing*, 23, 15–35.

Dekker, A. G., Zamurovic-Nenad, Z., Hoogenboom, H. J., and Peters, S. W. M. (1996). Remote sensing, ecological water quality modelling and in situ measurements: A case study in shallow lakes. *Hydrological Sciences*, 41, 531–547.

Del Castillo, C. E. (2005). *Remote sensing of coastal aquatic enironments*. Dordrecht, the Netherlands: Springer.

Del Castilo, C. E., and Miller, R. L. (2008). On the use of ocean color remote sensing to measure the transport of dissolved organic carbon by the Mississippi River plume. *Remote Sensing of Environment*, 112, 836–844.

Dewindar, K., and Khedar, A. (2001) Water quality assessment with simultaneous Landsat-5 TM at Manzala Lagoon, Egypt. *Hydrobiologia*, 457, 49–58.

Domagalski, J., Lin, C., Luo, C., Kang, J., Wang, S. M., Brown, L. R., and Munn, M. D. (2007). Eutrophication study at the Panjakou-Daheiting reservoir system, Northern Hebei Province, People's Republic of China: Chlorophyll-*a* model and sources of phosphorous and nitrogen. *Agricultural Water Management*, 94, 43–53.

Donlon, C. J. (2003). *The GHRSST–PP development and implementation plan, version 4*. Exeter, England: GHRSST-PP ProjectOffice, Met Office.

Donlon, C. J., Rayaner, N., Robinson, I., Poulter, D. J. S., Casey, K. S., Vazquez-Cuervo J., Armstrong, E., Bingham, E., Arino, O., Gentemann, C., May, D., Leborgne, P., Piolle, J., Barton, I., Beggs, H., Merchant, C. J., Heinz, S., Harris, A., Wick, G., Emery, B., Minnett, P., Evans, R., Liewellyn-Jones, D., Mutlow, C., Reynolds, R. W., and Kavamura, H. (2007). The global ocean data assimilation experiment high-resolution sea surface temperature pilot project. *Bulletin of the American Meteorological Society*, 88, 1197–1213.

Duan, H., Ma, R., Xu, J., Zhang, Y., and Zhang, B. (2010). Comparison of different semi-empirical algorithms to estimate chlorophyll-*a* concentration in inland lake water. *Environmental Monitoring and Assessment*, 170, 231–244.

Ekercin, S. (2007). Water quality retrievals from high resolution Ikonos multispectral imagery: A case study in Istanbul, Turkey. *Water, Air, and Soil Pollution*, 183, 239–251.

El Masri, B., and Rahman, A. F. (2008). *Estimation of water quality parameters for Lake Kemp Texas derived from remotely sensed data*. Retrieved from http://twri.tamu.edu/funding/usgs/2006–07/el-masri_manuscript.pdf

Emery, W. J., Yu, Y., Wick, G. A., Schluessel, P., and Reynolds, R. W. (1994). Correcting infrared satellite estimate of sea surface temperature for atmosphere water vapor attenuation. *Journal of Geophysical Research*, 99, 5219–5236.

Engman, E. T. (2009). *Remote sensing application for direct measurement of water quality*. Water Quality Algorithm Development Workshop, GEO Water Quality Working Group.

Falconer, I. (Ed.). (1993). *Algal toxins in seafood and drinking water*. New York, NY, Academic Press.

Falconer, I. (1996). Potential impact on human health of toxic cyanobacteria. *Phycologia*, 35(Suppl 6), 6–11.

Ferrari, G. M. (2000). The relationship between chromophoric dissolved organic matter and dissolved organic carbon in the European Atlantic Coastal Area and in the West Mediterranean Sea (Gulf of Lions). *Marine Chemistry*, 70, 339–357.

Ferrari, G. M., Dowell, M. D., Grossi, S., and Targa, C. (1996). Relationship between the optical properties of chromophoric dissolved organic matter and total concentration of dissolved organic carbon in Southern Baltic region. *Mar. Chem.* 55, 299–316.

Field, C. B., Behrenfeld, M. J., Randerson, J. T., and Falkowski, P. (1998). Primary production of the biosphere: Integrating terrestrial and oceanic components. *Science*, 281, 237–240.

Fukushima, H., Higurashi, A., Mitomi, Y., Nakajima, T., Noguchi, T., Tanaka, T., and Toratani, M. (1998). Correction of atmospheric effects on ADEOS/OCTS ocean color data: Algorithm description and evaluation of its performance. *Journal of Oceanography*, 54, 417–430.

Ganf, G., Oliver, R., and Walsby, A. (1989). Optical properties of gas-vacuolate cells and colonies of microcystis in relation to light attenuation in a turbid, stratified reservoir (Mount Bold Reservoir, South Australia). *Australian Journal of Freshwater Research*, 40, 595–611.

Genderen, J., and Pohl, C. (1994). *Image fusion: Issues, techniques, and applications. Intelligent Image Fusion*. Paper presented at the EARSel Workshop, Strasbourg, France.

Giardino, C., Brando, V. E., Dekker, A. G., Strombeck, N., and Candiani, G. (2007). Assessment of water quality in Lake Garda (Italy) using Hyperion. *Remote Sensing of Environment*, 109, 183–195.

Giardino, C., Pepe, M., Brivio, P. A., Ghezzi, P., and Zilioli, E. (2001). Detecting chlorophyll, Secchi disk depth and surface temperature in a sub-alpine lake using Landsat imagery. *Science of the Total Environment*, 268, 19–29.

Gilbes, F., López, J. M., and Yoshioka, P. M. (1996). Spatial and temporal variations of phytoplankton chlorophyll-a and suspended particulate matter in Mayagüez Bay, Puerto Rico. *Journal of Plankton Research*, 18, 29–43.

Glasgow, H. B., Burkholder, J. M., Reed, R. E., Lewitus, A. J., and Kleinman, J. E. (2004). Real-time remote monitoring of water quality: A review of current applications, and advancements in sensor, telemetry, and computing technologies. *Journal of Experimental Marine Biology and Ecology*, 300, 409–448.

Gomez, J. A. D., Alonso, C. A., and Garcia, A. A. (2011). Remote sensing as a tool for monitoring water quality parameters for Mediterranean lakes of European Union Water Framework Directive (WFD) and as a system of surveillance of cyanobacterial harmful algae bloom (SCyanoHABs). *Environmental Monitoring and Assessment*, 181, 317–334.

Gomez, R. A. (2000). Detection of total suspended sediments in the North Sea using AVHRR and ship data. *International Journal of Remote Sensing*, 21, 1583–1596.

Goodman, R. (1994). Overview and future trends in oil spill remote sensing. *Spill Science and Technology Bulletin*, 1, 11–21.

Gordon, H. R. (1978). Removal of atmospheric effects from satellite imagery of the oceans. *Applied Optics*, 17, 1631–1636.

Gordon, H. R. (1980). A preliminary assessment of the NIMBUS-7 CZCS atmospheric correction algorithm in a horizontally inhomogenous atmosphere. In J. F. R. Gower (Ed.), *Oceanography from space* (pp. 281–294). New York: Plenum Press.

Gordon, H. R., and Clark, D. K. (1980). Atmospheric effects in the remote sensing of phytoplankton pigments. *Boundary-Layer Meteorology*, 18, 299–313.

Gordon, H. R., and McCluney, W. R. (1975). Estimation of the depth of sunlight penetration in the sea for remote sensing. *Applied Optics*, 14, 413–416.

Gordon, H. R., and Wang, M. (1994). Retrieval of water-leaving radiance and aerosol optical thickness over the oceans with SeaWiFS: A preliminary algorithm. *Applied Optics*, 33, 443–452.

Ha, J., Hidaki, T., and Tsuno, H. (2011). Analysis of factors affecting the ratio of microcystin to chlorophyll-*a* in cyanobacterial blooms using real-time polymerase chain reaction. *Environmental Toxicology*, 26(1), 21–28.

Hanson, C. E., Waite, A. M., Thompson, P. A., and Pattiaratchi, C. B. (2007). Phytoplankton community structure and nitrogen nutrition in Leeuwin current and coastal waters of the Gascoyne Region of Western Australia. *Deep Sea Research II*, 54, 902–924.

He, B., Oki, K., Wang, Y., Oki, T., Yamashiki, Y., Takara, K., Miura, S., Imai, A., Oki, K., Komatsu, K., and Kawasaki, N. (2010). Estimation of monthly potential nitrogen load from agricultural and forest watersheds using quickbird remote sensing imagery. International Archives of the Photogrammetry, Remote Sensing and Spatial Information Science, Volume XXXVIII, Part 8, Kyoto Japan.

He, W., Chen, S., Liu, X., and Chen, J. (2008). Water quality monitoring in slightly-polluted inland water body through remote sensing: A case study in Guanting Reservoir, Beijing, China. *Frontiers of Environmental Science and Engineering in China Tidal Chlorophyll-a Variation in Estuaries*, 6, 1685–1706.

Heiskary, S., and Wilson, B. (2005). *Minnesota lake water quality: Developing nutrient criteria* (3rd ed.). St. Paul MN: Minnesota Pollution Control Agency.

Hitzfield, B., Hoger, S., and Dietrich, D. (2000). Cyanobacterial toxins: Removal during drinking water treatment and human risk assessment. *Environmental Health Perspectives*, 108, 113–122.

Hoogenboom, H. J., Dekker, A. G., and De Haan, J. F. (1998). Retrieval of chlorophyll and suspended matter from imaging spectrometry data by matrix inversion. *Canadian Journal of Remote Sensing*, 24, 44–152.

Huang, Y., Jiang, D., Zhuang, D., and Fu, J. (2010). Valuation of hyperspectral indices for chlorophyll-a concentration estimation in Tangxun Lake (Wuhan, China). *International Journal of Environmental Research and Public Health*, 7, 2437–2451.

Hunter, P. D., Tyler, A. N., Wilby, N. J., and Gilvear, D. J. (2008). The spatial dynamics of vertical migration by microcystis aeruginosa in a eutrophic shallow lake: A case study using high spatial resolution time-series airborne remote sensing. *Limnology and Oceanography*, 53, 2391–2406.

Jaquet, J. M., Schenaz, F., Bossard, P., Hanselmann, K., and Gendre, F. (1994). Measurements and significance of bio-optical parameters for remote sensing in two subalpine lakes of different trophic state. *Aquatic Sciences*, 56, 263–305.

Jiao, H. B., Zha, Y., Gao, J., Li, Y. M., Wei, Y. C., and Huang, J. Z. (2006). Estimation of chlorophyll-*a* concentration in Lake Tai, China using in situ hyperspectral data. *International Journal of Remote Sensing*, 27, 4267–4276.

Jones, G., and Orr, P. (1994). Release and degradation of microcystin following algaecide treatment of a microcystis aeruginosa bloom in a recreational lake, as 248 determined by HPLC and protein phosphate inhibition assay. *Water Resources*, 28, 871–876.

Kallio, K., Kutser, T., Hannonen, T., Koponen, S., Pulliainen, J., Vepsalainen, J., and Pyhalahti, T. (2001). Retrieval of water quality from airborne imaging spectrometry of various lake types in different seasons. *Science of the Total Environment*, 268, 59–77.

Kallio, K., Pulliainen, J., and Ylostalo, P. (2005) MERIS, MODIS and ETM+ channel configurations in the estimation of lake water quality from subsurface reflectance using semi analytical and empirical algorithms. *Geophysica*, 41, 31–55.

Katlane, R., Dupouy, C., and Zargouni, F. (2012). Chlorophyll and turbidity concentration as an index of water quality of the Gulf of Gabes from MODIS in 2009. *Revue Teledetection*, 11, 263–271.

Keiner, L. E., and Yan, X. H. (1998). A neural network model for estimating sea surface chlorophyll and sediments from thematic mapper imagery. *Remote Sensing Environment*, 66, 63–165.

Kirk, J. T. O. (1981). Estimation of scattering coefficient of natural water using underwater irradiance measurements. *Australian Journal of Marine and Freshwater Research*, 32, 533–539.

Kishino, M., Ishimaru, T., Furuya, K., Oishi, T., and Kawasaki, K. (1998). In-water algorithms for ADEOS/OCTS. *Journal of Oceanography*, 54, 431–436.

Knobeloch, L., Salna, B., Hogan, A., Postle, J., and Anderson, H. (2000). Blue babies and nitrate-contaminated well water. *Environmental Health Perspectives*. 108, 675–678.

Kopelevich, O. V., Sheberstov, S. V., Yunev, O., Basturk, O., Finenko, Z. Z., Nikonov, S., and Vedernikov, V. J. (2002). Surface chlorophyll in the Black Sea over 1978–1986 derived from satellite and in situ data. *Journal of Marine Systems*, 36, 145–160.

Kutser, T., Pierson, D. C., Tranvik, L., Reinart, A., Sobek, S., and Kallio, K. (2005). Using satellite remote sensing to estimate the colored dissolved organic matter absorption coefficient in lakes. *Ecosystems*, 8, 709–720.

Lapucci, C., Rella, M. A., Brandini, C., Ganzin, N., Gozzini, B., Maselli, F., Massi, L., Nuccio, C., Ortolani, A., and Trees, C. (2012). Evaluation of empirical and semi-analytical chlorophyll algorithms in the Ligurian and North Tyrrhenian Seas. *Journal of Applied Remote Sensing*, 6, 063565.

Li, L., Sengpiel, R. E., Pascual, D. L., Tedesco, L. P., Wilson, J., and Soyeux, E. (2010). Using hyperspectral remote sensing to estimate chlorophyll-*a* and phycocyanin in a Mesotrphic reservoir. *International journal of Remote Sensing*, 31, 4147–4162.

Liew, S. C. (n.d.). *Retrieving optical parameters of coastal waters using Hyperion data*. Retrieved from http://eo1.gsfc.nasa.gov/new/validationreport/Technology/Documents/Tech.Val.Report/Science_Summary_Liew_1.pdf

Lindell, T., Pierson, D., Premazzi, G., and Zilioli, F. (1999). *Manual for monitoring European lakes using remote sensing techniques*. EUR 18665 EN. Luxembourg: European Communities.

Liu, D., Zhang, Y., Zhang, B., Song, K., Wang, Z., Duan, H., and Li, F. (2006). Effects of sensor noise in spectral measurements on chlorophyll-a retreival in Nanhu Lake of Changchun, China. *Journal of Electromagnetic Waves and Application*, 20, 547–557.

Liu. Y., Islam, M. A., and Gao, J. (2003). Quantification of shallow water quality parameters by means of remote sensing. *Progress in Physical Geography*, 27, 24–43.

Lodhi, M. A., Rundquist, D. C., Han, L., and Kuzila, M. S. (1998). Estimation of suspended sediment concentration in water using integrated surface reflectance. *Geocarto International*, 13(2), 11–15.

Ma, R., and Dai, J. (2005). Investigation of chlorophyll-a and total suspended matter concentrations using Landsat ETM and field spectral measurement in Taihu Lake, China. *International Journal of Remote Sensing*, 26, 2779–2787.

Ma, R., Tang, J., and Dai, J. (2006). Bio-optical model with optimal parameter suitable for Taihu lake in water color remote sensing. *Journal of Remote Sensing*, 27, 4305–4328.

Makkeasorn, A., Chang, N. B., Beaman, M., Wyatt, C., and Slater, C. (2006). Soil moisture prediction in a semi-arid reservoir watershed using RADARSAT satellite images and genetic programming. *Water Resources Research*, 42, 1–15.

Mancino, G., Nole, A., Urbano, V., Amato, M., and Ferrara, A. (2009). Assessing water quality by remote sensing in small lakes: The case study of Monticchio Lakes in Southern Italy. *iForest*, 2, 154–161.

Mannino, A., Russ, M. E., and Hooker, S. B. (2008). Algorithm development and validation for satellite-derived distributions of DOC and CDOM in the U.S. Middle Atlantic bight. *Journal of Geophysical Research: Oceans*, 113, C07051.

Maritorena, S., and Siegel, D. A. (2005). Consistent merging of satellite ocean color datasets using a bio-optical model. *Remote Sensing of Environment*, 94, 429–440.

Maritorena, S., Siegel, D., and Peterson, A. (2002). Optimization of a semianalytical ocean color model for global-scale applications. *Applied Optics*, 41, 2705–2714.

Matsuoka, A., Hooker, S. B., Bricaud, A., Gentili, B., and Babin, M. (2012). Estimating absorption coefficients of colored dissolved organic matter (CDOM) using a semi-analytical algorithm for Southern Beaufort Sea (Canadian Arctic) Waters:

Application to deriving concentrations of dissolved organic carbon from space. *Biogeosciences Discussions*, 9, 13743–13771.

Maurer, J. (2002). *Infrared and microwave remote sensing of sea surface temperature (SST)*. Overview of a seminar given by Dr. Gary, A. Wick of NOAA Environementtal Technology Laboratory.

McClain, C. R., Feldman, G. C., and Hooker, S. B. (2004). An overview of the SeaWiFS project and strategies for producing a climate research quality ocean bio-optical time series. *Deep Sea Research II*, 51, 5–42.

McClain, C. R., and Meister, G. (2012). IOCCG Working Group on Mission Requirements for Future Ocean-Colour Sensors, Mission Requirements for Future Ocean-Colour Sensors Reports of the International Ocean-Colour Coordinating Group, Report 13,CreSOS, Udayana University, Denpasar, Indonesia http://www.ioccg.org/reports/IOCCG_Report13.pdf.

Menken, K., Brozonik, P., and Bauer, M. (2005). *Influence of chlorophyll and colored dissolved organic matter (CDOM) on lake reflectance spectra: Implications for measuring lake properties by remote sensing*. University of Minnesota.

Merchant, C. J., Borgne, P. L., Marsouin, A., and Roquet, H. (2008). Optimal estimation of sea surface temperature from split-window observations. *Remote Sensing of Environment*, 112, 2469–2484.

Minnesota Pollution Control Agency. (2008). *Nutrients: Phosphorus, nitrogen sources: A general overview*. Water quality/Impaired Waters#3.22.

Minnett, P. J., and Barton, I. J. (2010). Remote sensing of the earth's surface temperature. In Z. M. Zhang, B. K. Tsai, and G. Machin (Eds.), *Radiometric temperature measurements and applications* (pp. 333–391). New York: Academic Press.

Mole, J., Chow, C., Drikas, M., and Burch, M. (1997). *The influence of cultural media on growth and toxin production of the cyanobacterium* Microcystis aeruginosa *Kutz Emend Elenkin*. Paper presented at the 13th Annual Conference of the Australian Society for Psychology and Aquatic Botany, Hobart, Tasmania, January.

Morel, A., and Berthon, J. F. (1989). Surface pigments, algal biomass profile, and potential production of the eutrophis layer: Relationships reinvestigated in view of remote applications. *Limnology and Oceanography*, 34, 1545–1562.

Morel, A., Gentili, B., Chami, M., and Ras, J. (2006). Bio-optical properties of high chlorophyll case 1 waters of yellow-substance-dominated case 2 waters. *Deep Sea Research I*, 53, 1439–1459.

Morel, A., Huot, Y., Gentili, B., Werdell, J., Hooker, S. B., and Franz, B. A. (2007). Examining the consistency of products derived from various ocean color sensors in open ocean (Case 1) waters in the perspective of a multi-sensor approach. Remote Sensing of Environment. 111, 69–88.

Morel, A., and Prieur, L. (1977). Analysis of variations in ocean color. *Limnology and Oceanography*, 22, 709–722.

Moser, G., and Serpico, S. B. (2009). Automatic parameter for support vector regression for land and sea surface temperature estimation from remote sensing data. *Geoscience and Remote Sensing*, 47, 909–921.

Moses, W. J., Gitelson, A. A., Perk, R. L., Gurlin, D., Rundquist, D. C., Leavitt, B. C., Barrow, T. M., and Brakhage, P. (2012). Estimation of chlorophyll-*a* concentration in turbid productive waters using airborne hyperspectral data. *Water Research*, 46, 993–1004.

Muslim, I., and Jones, G. (2003). The seasonal validation of dissolved nutrients, chlorophyll-*a*, and suspended sediments at Nelly Bay, Magnetic Island. *Estuarine, Coastal, and Shelf Science*, 57, 445–455.

Myint, S. W., and Walker, N. D. (2002). Quantification of surface suspended sediments along a river dominated coast with NOAA AVHRR and SeaWiFS measurements; Louisiana, USA. *International Journal of Remote Sensing*, 23, 3229–3249.

Naderi, F., Freilich, M. H., and Long, D. G. (1991). Spaceborne radar measurement of wind velocity over the ocean: An overview of the NSCAT scatterometer system. *Proceedings of the IEEE*, 79, 850–866.

Nalli, N. R., and Smith, W. L. (1998). Improved remote sensing of sea surface skin temperature using a physical retrieval method. *Journal of Geophysical Research*, 103, 10527–10542.

National Academies. (2008). *21 century's grand engineering challenges* [Press Release]. Retrieved from http://www8.nationalacademies.org/onpinews/newsitem.aspx?RecordID=02152008

National Research Council. (2008). *Integrating multiscale observations of U.S. waters*. Washington DC: The National Academies Press.

Novo, E. M. M., Hansom, J. D., and Curran, P. J. (1989). The effect of sediment type on the relationship between reflectance and suspended sediment concentration. *International Journal of Remote Sensing*, 10, 1283–1289.

Pacciaroni, M., and Crispi, G. (2007). Chlorophyll signatures and nutrient cycles in the Mediterranean Sea: A model sensitivity study to nitrogen and phosphorous atmospheric inputs. *Biogeosciences Discussions*, 4, 909–959.

Panda, S. S., Garg, V., and Chaubey, I. (2004). Artificial neural networks application in lake water quality estimation using satellite imagery. *Journal of Environmental Informatics*, 4(2), 65–74.

Pavelsky, T. M., and Smith, L. C. (2009). Remote sensing of suspended sediment concentration, flow velocity, and lake recharge in the Peace-Athabasca Delta, Canada. *Water Resources Research*, 45, W11417.

Phillips, G., Lyche-Solheim, A., Skjelbred, B., Mischke, U., Drakare, S., Free, G., Järvinen, M., de Hoyos, C., Morabito, G., Poikane, S., and Carvalho, L. (2012). A phytoplankton trophic index to assess the status of lakes for the Water Framework Directive. *Hydrobiologia*. doi:10.1007/s10750-012-1390-8.

Phinn, S. R., Dekker, A. G., Brando, V. E., and Roelfsema, C. M. (2005). Mapping water quality and subtrate cover in optically complex coastal and reef waters: An integrated approach. *Marine Pollution Bulletin*, 51, 459–469.

Pulliainen, J., Kallio, K., Eloheimo, K., Koporen, S., Servomaa, H., Hannonen, T., Tauriainen, S., and Hallikainen, M. (2001). A semi-operative approach to lake water quality retrieval from remote sensing data. *Science of the Total Environment*, 268, 79–93.

Ramalingam, R. R. M., Ghosh, S. K., and Kothyari, U. C. (2008). Mapping of suspended sediments using site specific seasonal algorithms. *Journal of Indian Society of Remote Sensing*, 36, 61–68.

Randolph, K., Wilson, J., Tedesco, L., Li, L., Pascual, D. L., and Soyeux, E. (2008). Hyperspectral remote sensing of cyanobacteria in turbid productive water using optically active pigments, chlorophyll-*a* and phycocyanin. *Remote Sensing of Environment*, 112, 4009–4019.

Reif, M. (2011). *Remote sensing for inland water quality monitoring: A U.S. monitoring*. Washington, DC: U.S. Army Corps of Engineers.

Reinart, A., and Reinhold, M. (2008). Mapping surface temperature in large lakes with MODIS data. *Remote Sensing of Environment*, 112, 603–611.

Richards, J. (1986). *Remote sensing digital image analysis: An introduction*. New York: Springer-Verlag.

Riha, S., and Krawczyk, H. (2011). *Development of a remote sensing algorithm for cyanobacterial phycocyanin pigment in the Baltic Sea using neural network approach*. Proceedings of SPIE 8175, Remote Sensing of the Ocean, Sea Ice, Coastal Waters, and Large Water Regions, 817504.

Rinta-Kanto, J., Konopko, E., DeBruyn, J., Bourbonniere, R., Boyer, G., and Wilhelm, S. (2009). Lake Erie microcystis: Relationship between microcystin production, dynamics of genotypes and environmental parameters in a large lake. *Harmful Algae*, 8, 665–673.

Ritchie, J. C., and Cooper, C. M. (n.d.). *Remote sensing techniques for determining water quality: Applications to TMDLs*. Retrieved from http://www.geo.tu-freiberg.de/studenten/Baikal_2004/remote_water_quality.pdf

Ritchie, J. C., Cooper, C. M., and Schiebe, F. R. (1990). The relationship of MSS and TM digital data with suspended sediments, chlorophyll, and temperature in Moon Lake, Mississippi. *Remote Sensing of Environment*, 33, 137–148.

Ritchie, J. C., and Schiebe, F. R. (1986). Monitoring suspended sediments with remote sensing techniques. *Hydrologic Application of Space Technology*, 160, 233–243.

Ritchie, J. C., Schiebe, F. R., and McHenry, J. R. (1976). Remote sensing of suspended sediment in surface water. *Photographic Engineering Remote Sensing*, 42, 1539–1545.

Ritchie, J. C., Zimba, P. V., and Everitt, J. H. (2003). Remote sensing techniques to assess water quality. *Photogrammetric Engineering and Remote Sensing*, 69, 695–704.

Robinson, I. S. (2004). *Measuring the oceans from space: The principles and methods of satellite oceanography*. Chichester, England: Praxis.

Rochelle-Newall, E. J., and Fisher, T. R. (2002). Chromophoric dissolved organic matter and dissolved organic carbon in Chesapeake Bay. *Marine Chemistry*, 77, 23–41.

Rodríguez-Guzmán, V., and Gilbes-Santaella, F. (2009). Using MODIS 250 m Imagery to Estimate Total Suspended Sediment in a Tropical Open Bay. *International Journal of Systems Applications, Engineering, and Development*, 1(3), 36–44.

Rogalus, M., and Watzin, M. (2008). Evaluation of sampling and screening techniques for tiered monitoring of toxic cyanobacteria in lakes. *Harmful Algae*, 7, 504–514.

Salma, M. S., Dekker, A., Su, Z., Mannerts, C. M., and Verhoef, W. (2009). Deriving inherent optical properties and associated inversion-Uncertainties in the Dutch Lakes. *Hydrology and Earth System Sciences*, 13, 1113–1121.

Savage, C., Leavitt, P. R., and Elmgren, R. (2010). Effects of landuse, urbanization and climate variability on coastal eutrophication in the Baltic Sea. *Limnology and Oceanography*, 55, 1033–1046.

Schultz, G. (1988). Remote sensing in hydrology. *Journal of Hydrology*, 100, 239–265.

Senay, G. B., Shafique, N. A., Autrey, B. C., Fulk, F., and Cormier, S. M. (2001). The selection of narrow wavebands for optimizing water quality monitoring on the Great Miami River, Ohio using hyperspectral remote sensor data. *Journal of Spatial Hydrology*, 1, 1–22.

Shubha, S. (2000). *Remote sensing of ocean colour in coastal, and other optically-complex, waters.* : International Ocean-Colour Coordinating Group, Busan, South Korea. http://www.ioccg.org/reports/report5.pdf

Siegel, D. A., Thomas, A. C., and Marra, J. (2004). Views of ocean process from the sea-viewing wide field-of-view sensor (SeaWiFS) mission: Introduction to the second special issue. *Deep-Sea Research II*, 51, 911–912.

Simis, S. G. H., Peters, S. W. M., and Gons, H. J. (2005). Remote sensing of the cyanobacterial pigment phycocyanin in turbid inland water. *Limnology and Oceanography*, 50, 237–245.

Smith, R. B. (2012). *Introduction to remote sensing of environment (RSE)*, MicroImages, Inc., Nebraska, U.S.A.

Smith, W. L., Khuteson, R. O., Revercomb, H. E., Feltz, W., Howell, H. B., Menzel, W. P., Nalli, N. R., Brown, J., Minnett, P., and McKeown, W. (1996). Observation of the infrared radiative properties of the ocean implications for the measurement of sea surface temperature via satellite remote sensing. *Bulletin of the American Meteorological Society*, 77, 41–51.

Smyth, T. J., Moore, G. F., Hirata, T., and Aiken, J. (2006). Semi-analytical model for the derivation of ocean color inherent optical properties: Description, implementation, and performance assessment. *Applied Optics*, 45, 8116–8131.

Song, K., Li, L., Tedesco, L., Clercin, N., Hall, B., Li, S., Shi, K., Liu, D., and Sun, Y. (2013). Remote estimation of phycocyanin (PC) for inland waters coupled with YSI PC fluorescence probe. *Environmental Science and Pollution Research*, 20, 5330–5340.

Song, K., Lu, D., Li, L., Li, S., Wang, Z., and Du, J. (2012). Remote sensing of chlorophyll-*a* concentration for drinking water source using genetic algorithms (GA): Partial least square (PLS) modeling. *Ecological Informatics*, 10, 25–36.

Stramski, D., Reynolds, R., Kahru, M., and Mitchell, B. (1999). Estimation of particulate organic carbon in the ocean from satellite remote sensing. *Science*, 285(5425), 239–242.

Sudheer, K. P., Chaubey, I., and Garg, V. (2006). Lake water quality assessment from Landsat TM data using neural network: An approach to optimal band combination selection. *Journal of American Water Resources Society*, 42, 1683–1695.

Theimann, S., and Kaufmann, M. (2002). Lake water quality monitoring using hyperspectral airborne data-A semi-empirical multisensor and multitemporal approach for the Mevklenburg Lake District, Germany. *Remote Sensing of Environment*, 81, 228–237

Topouzelis, K. N. (2008). Oil spill detection by SAR images: Dark formation detection, feature extraction, and classification algorithms. *Sensors*, 8, 6642–6659.

Torbick, N., Hu, F., Zhang, J., Qi, J., Zhang, H., and Becker, B. (2008). Mapping chlorophyll-a concentrations in West Lake, China using Landsat 7 ETM+. *Journal of Great Lakes Research*, 34, 559–565.

Torgersen, C. E., Faux, R. N., McIntosh, B. A., Poage, N. J., and Norton, D. J. (2001). Airborne thermal remote sensing for water temperature assessment in rivers and streams. *Remote Sensing of Environment*, 76, 386–398.

Tyler, A. N., Svab, E., Preston, T., Presing, M., and Kovacs, W. A. (2006). Remote sensing of the water quality of shallow lakes: A mixture modeling approach to quantifying phytoplankton in water characterized by high-suspended sediment. *International Journal of Remote Sensing*, 27, 1521–1537.

Tzortziou, M., Subramaniam, A., Herman, J. R., Gallegos, C. L., Neale, P. J., and Harding, L. W. Jr. (2007). Remote sensing reflectance and inherent optical properties in the Mid Chesapeake Bay, *Estuarine Coastal and Shelf Science*, 72, 16–32.

U.S. Environmental Protection Agency. (2002). *Nitrogen: Multiple and regional impacts*. EPA-430-R-01-006. Washington, DC: U.S. EPA.

U.S. Environmental Protection Agency. (2009). *The National Water Quality Inventory: Report to Congress for the 2004 reporting cycle: A profile*. Retrieved from http://water.epa.gov/lawsregs/guidance/cwa/305b/2004report_index.cfm

Usali, N., and Ismail, M. H. (2010). Use of remote sensing and GIS in monitoring water quality. *Journal of Sustainable Development*, 3, 228–238.

Van Der Woerd, H., Hakvoort, J. H. M., Hoogenbppm, H. J., Ontzigt, N., Pasterkam, R., Peters, S. W. M., Ruddick, K. G., De Valk, C., and Vos, R. J. (2000). *Towards an operational monitoring system for turbid water*. Amsterdam, the Netherlands: IVM/VU.

Vertucci, F., and Likens, G. E. (1989). Spectral reflectance and water quality of Adirondack Mountain Region lakes. *Limnology and Oceanography*, 34, 1656–1672.

Vincent, R., Xiaoming, Q., McKay, R., Miner, J., Czajkowski, K., Savino, J., and Bridgeman, T. (2004). Phycocyanin detection from Landsat TM data for mapping cyanobacterial blooms in Lake Erie. *Remote Sensing of the Environment*, 89, 381–392.

Vodacek, K. A., Hoge, F. E., Swift, R. N., Yungel, J. K., Peltzer, E. T., and Blough, N. V. (1995). The use of in-situ and airborne fluorescence measurement to determine UV absorption coefficients and DOC concentrations in surface water. *Limnology and Oceanography*, 40, 411–415.

Wallace, B. (2003). *TOC analysis of humic acid: Sample preparation is the key*. Teledyne Technologies Company.

Walton, C. C. (1988). Nonlinear multichannel algorithms for estimating sea surface temperature with AVHR satellite data. *Journal of Applied Meteorology*, 27, 115–124.

Wang, F., Zhou, B., Liu, X., Zhou, G., and Zhao, K. (2012). Remote sensing inversion model of surface water suspended sediment concentration based on in situ measured spectrum in Hangzhou Bay, China. *Environmental Earth Sciences*, 67, 1669–1677.

Wang, H., Fan, T., Shi, A., Huang, F., and Wang, H. (2010). Fuzzy integral based information fusion for water quality monitoring using remote sensing data. *International Journal of Communications, Network and System Science*, 3, 737–744.

Wang, J. P., Cheng, S. T., and Jia, H. F. (2008). *Application of artificial neural network technology in water color remote sensing inversion of inland waterbody using TM data*. The International Archives of Photogrammetry. Remote Sensing and Spatial Information Sciences. Istanbul, Turkey: ISPRS Congress, Proceedings of Commission IV.

Wang, M. (2010). *Atmospheric correction for remotely-sensed ocean-colour products.*: International Ocean-Colour Coordinating Group, Rio de Janeiro, Brazil. http://www.ioccg.org/reports/report10.pdf

Wang, P., Boss, E., and Roesler, C. (2005). Uncertainties of inherent optical properties obtained from semianalytical inversions of ocean color. *Applied Optics*, 44, 4074–4084.

Wang, Y., Yan, F., Zhang, P., and Dong, W. (2007). Experimental research on quantitative inversion models of suspended sediment concentration using remote sensing technology. *Chinese Geographical Science*, 17, 243–249.

World Health Organization. (1999). *Toxic cyanobacteria in water: A guide to their public health consequences, monitoring and management*. London, England: E & FN Spon.

Wu, C., Wu, J., Qi, J., Zhang, L., Huang, H., Lou, L., and Chen, Y. (2010). Empirical estimation of total phosphorous concentration in the mainstream of the Qiantang River in China using Landsat TM data. *International Journal of Remote Sensing*, 31, 2309–2324.

Wynne, T., Stumpf, R., Tomlinson, M., Warner, R., Tester, P., Dyble, J., and Fahnenstiel, G. (2008).Relating spectral shape to cyanobacterial blooms in the Laurentian Great Lakes. *International Journal of Remote Sensing*, 29, 366–3672.

Xing, X. G., Zhao, D. Z., Liu, Y. G., Yang, J. H., Xiu, P., and Wang, L. (2007). An overview of remote sensing of chlorophyll fluorescence. *Ocean Science Journal*, 42, 49–59.

Yacobi, Y. Z., Gitelso, A., and Mayo, M. (1995). Remote sensing of chlorophyll in Lake Kinneret using high-spectral-resolution radiometer and Landsat TM: Spectral features of reflectance and algorithm development. *Journal of Plankton Research*, 17, 2155–2173.

Yang, M. D., Merry, C. J., and Sykes, R. M. (1999). Integration of water quality modeling, remote sensing and GIS. *Journal of American Water Resources Association*, 35, 253–263.

Yu, T. (2005). *Utility of remote sensing data in retrieval of water quality constituents concentrations in coastal water of New Jersey*. Doctoral dissertation, New Jersey Institute of Technology.

Zhang, T., and Frank, F. (2004). An approach to improving the retrieval accuracy of oceanic constituents in case II waters. *Journal of Ocean University of China*, 3, 220–224.

Zhang, Y., Pulliainen, J., Koporen, S., and Hallikainen, M. (2002). Application of an empirical neural network to surface water quality estimation in the Gulf of Finland using combined optical data and microwave data. *Remote Sensing of Environment*, 81, 327–336.

Zhang, Y., Pullianen, J. T., Koponen, S. S., and Hallikainen, M. T. (2003). Water quality retrievals from combined Landsat TM data and ERS-2 SAR data in the Gulf of Finland. *IEEE TRANSACTIONS ON GEOSCIENCE AND REMOTE SENSING*, 41, 622–629.

Zhou, X. B., Chang, N. B., and Li, S. S. (2007). Detection of coastal region sea ice decay from orthorectified RADARSAT-1 ScanSAR imagery: A case study of Bering Strait and Norton Sound, Alaska. *Journal of Environmental Informatics*, 10, 37–46.